

DESIGN OF A VOLTAMMETRY SYSTEM FOR IN VIVO MEASUREMENT OF DOPAMINE CONCENTRATION

A THESIS SUBMITTED TO
THE GRADUATE SCHOOL OF
ENGINEERING AND NATURAL SCIENCES
OF ISTANBUL MEDIPOL UNIVERSITY
IN PARTIAL FULFILLMENT OF THE REQUIREMENTS FOR
THE DEGREE OF
MASTER OF SCIENCE
IN
BIOMEDICAL ENGINEERING AND BIOINFORMATICS

By
Raheel Riaz
June, 2018

DESIGN OF A VOLTAMMETRY SYSTEM FOR IN VIVO MEASUREMENT OF DOPAMINE CONCENTRATION

By Raheel Riaz

June, 2018

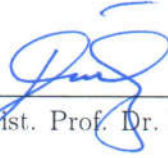
We certify that we have read this thesis and that in our opinion it is fully adequate, in scope and in quality, as a thesis for the degree of Master of Science.



Assist. Prof. Dr. Mehmet Kocatürk(Advisor)



Assoc. Prof. Dr. Yasemin Yüksel Durmaz



Assist. Prof. Dr. Pınar Öz

Approved by the Graduate School of Engineering and Natural Sciences:



Prof. Dr. Talip Alp

Director of the Graduate School of Engineering and Natural Sciences

I hereby declare that all information in this document has been obtained and presented in accordance with academic rules and ethical conduct. I also declare that, as required by these rules and conduct, I have fully cited and referenced all material and results that are not original to this work.

Name, Last Name: RAHEEL RIAZ

Signature : 

ABSTRACT

DESIGN OF A VOLTAMMETRY SYSTEM FOR IN VIVO MEASUREMENT OF DOPAMINE CONCENTRATION

Raheel Riaz

M.S. in Biomedical Engineering and Bioinformatics

Advisor: Assist. Prof. Dr. Mehmet Kocatürk

June, 2018

Dopamine has a critical role in motor control, motor learning, reinforcement learning, cognition, attention and motivation. Consequently, the physiology of the dopaminergic system is an important and highly active research topic. Fast-scan cyclic voltammetry (FSCV) technique enables in vivo measurement of dopamine concentration with high, subsecond temporal resolution. In this study, our aim was to propose a low-cost and practical FSCV system that enables the recording of the phasic changes in dopamine concentration in the rat brain during behavioral experiments. We developed the voltammetry hardware using a microcontroller and a combination of analog integrated circuits (ICs) to generate a triangular voltametric waveforms phase-locked to mains frequency and to apply these waveforms to a carbon fiber microsensor. The voltammetric current through the microsensor is converted to voltage, amplified, filtered using the hardware and then fed to a data acquisition card on a PC. A LabVIEW application is also developed to control the data acquisition hardware, digital filtering of the recorded signals and storage of the data. In order to validate the practicality of the system, we chronically implanted one rat with carbon fiber microsensor in the ventromedial striatum (VMS) and recorded the voltammetric signals 1) in response to presentation of unexpected primary rewards (unconditioned stimuli), 2) in response to presentation of reward predictive stimuli (cue light) and 3) during electrical stimulation of dopaminergic pathway. Based on 5 recording sessions in which unexpected rewards were presented and 5 recording sessions in which predictive stimuli were presented, the phasic increase in the dopamine concentration was measured as 50.5 ± 13.1 nM and 40.2 ± 13.9 nM, respectively. The peak increase in dopamine concentration with electrical stimulation of the dopaminergic pathway during implantation surgery was measured as 132.8 nM. Our results based

on the recordings from one rat indicate that phasic increases in dopamine concentration in the VMS in response to delivery of unexpected rewards and reward predictive stimuli can be detected using the proposed system. The cost of the present FSCV system is approximately \$1200.



Keywords: Dopamine, Voltammetry, FSCV, VMS, LabVIEW.

ÖZET

İN VİVO DOPAMİN KONSANTRASYONU ÖLÇÜMÜ İÇİN VOLTAMETRİ SİSTEMİ TASARIMI

Raheel Riaz

Biyomedikal Mühendisliği ve Biyoinformatik, Yüksek Lisans

Tez Danışmanı: Dr. Öğr. Üyesi Mehmet KOCATÜRK

Haziran, 2018

Dopamin motor control, motor öğrenme, pekiştirmeli öğrenme, bilişsellikte, dikkat ve motivasyonda kritik öneme sahiptir. Bu yüzden dopaminerjik sistem fizyolojisi önemli ve aktif bir araştırma konusudur. Hızlı tarama döngüsel voltametri (HTDV) tekniği yüksek, saniye alt zamansal çözünürlükle in vivo dopamin konsantrasyonu ölçümlerini mümkün hale getirmektedir. Bu çalışmadaki amacımız davranış deneyleri sırasında sıçan beyinde dopamin konsantrasyonu değişimlerinin kaydedilmesini mümkün hale getiren düşük maliyetli ve uygulanabilir bir HTDV sistemi geliştirmektir. Şebeke frekansı fazla kilitlenmiş gen ekilli dalgalar retmek ve bu dalgalar mikroalgılayıcıya uygulayabilmek için voltametri donanımı bir mikrodenetleyici ve analog entegre devrelerin bir kombinasyonunu kullanarak geliştirdik. Mikroalgılayıcı aracılığıyla alınan voltametrik akım bu donanımla voltaja çevrilmekte, kuvvetlendirilmekte, filtrelenmekte ve ardından PC üzerindeki bir veri toplama kartına iletilmektedir. Veri toplama kartını kontrol etmek, sayısal filtreleme yapmak ve veri kaydı için de bir LabVIEW uygulaması geliştirdik. Sistemin uygulanabilirliğini doğrulamak için sıçan ventromedial striatumuna (VMS) kronik olarak karbon fiber mikroalgılayıcılar implante ettik ve 1) sıçana beklenmedik anlarda ödülleri verildiği, 2) ödülün kestirimcisi uyaranlar verildiği ve 3) dopaminerjik yolların elektriksel olarak uyarıldığı sırada voltametrik işretleri kaydettik. Beklenmedik ödülleri verildiği 5 deneme ve ödül kestirimcisi uyaranların verildiği 5 deneme sırasında alınan kayıtlara göre dopamin konsantrasyonundaki fazik artış sırasıyla 50.5 ± 13.1 nM and 40.2 ± 13.9 nM olarak ölçüldü. Dopaminerjik yolların implantasyon ameliyatı sırasında elektriksel olarak uyarıldığında en yüksek dopamin konsantrasyonu artışı 132.8 nM olarak ölçüldü. Bir sıçandan aldığımız kayıtlar önerdiğimiz sistemi kullanarak ventromedial striatumdaki fazik dopamin konsantrasyonu artışlarının beklenmedik ödülleri ve ödülün kestirimcisi uyaranlar verildiğinde tespit edilebileceğini

göstermiştir. Önerdiğimiz HTDV sistemin maliyeti yaklaşık olarak 1200 USD'dir.



Acknowledgement

I would like to thank to my thesis advisor Mehmet Kocatürk for his great advises and support from the beginning to the end of my master study. I had opportunity to ask any question related to my study, whenever I need. I appreciate for this continuous guidance.

Also, I am grateful to M. Sohaib Solaija for his guidance in writing this thesis, and other friends for their support that helped me to keep being in the way.

In the end I would like to give my biggest gratitude to my parents for pushing me always to reach my full potential and to achieve whatever I have achieved so far. ...

Contents

1	Introduction	1
1.1	Dopamine and the Dopaminergic System	2
1.1.1	Dopamine	2
1.1.2	Dopaminergic Pathways	3
1.1.3	Physiolgy of the Dopaminergic System	5
1.2	Fast Scan Cyclic Voltammetry (FSCV)	7
1.2.1	Voltammetry	7
1.2.2	Fast Scan Cyclic Voltammetry (FSCV)	8
1.2.3	Literature Review	9
1.3	Objective of Thesis	11
2	Methods	12
2.1	The Fast Scan Cyclic Voltammetry System	12
2.1.1	Hardware	12

2.1.2	The Software	20
2.2	The Microsensors, The Reference and Stimulation Electrodes . . .	24
2.2.1	Reference Electrodes	24
2.2.2	Stimulation Electrodes	25
2.2.3	Carbon Fiber Microsensor	26
2.3	Surgical Procedure	28
2.4	Experiments	30
3	Results	31
3.1	Voltammetric Recordings of Rat in Idle State	31
3.2	Voltammetric Recordings During Stimulation of the Dopaminergic Pathway	32
3.2.1	During Surgery	32
3.2.2	After Recovery	35
3.3	Recording During Behavioral Experiments (Pavlovian Conditioning)	38
4	Discussion	42
4.1	Advantages of the System	45
4.2	Limitations of the System and Future Improvements	46
A	Appendix	55

A.1 Amplifier Schematic 55

A.2 Pulse Generator Schematic 56

A.3 Integrator Schematic 57

A.4 PCB Layout 58



List of Figures

1.1	Molecular Structure of Dopamine [1]	3
1.2	The dopaminergic pathways in the rat brain	4
1.3	The principle of fast scan cyclic voltammetry	8
2.1	Basic structure of voltammetric hardware (modified from [2]). . .	13
2.2	The block diagram of voltammetric signal generator	13
2.3	Architecture of pulse generator block. Microcontroller generates unipolar pulse signal which is first isolated using optocoupler and then converted to bipolar pulse signal using analog comparator. .	14
2.4	The integrator circuit with constant capacitance and variable resistor. The resistance can be used to control the ramp of the triangular waveform.	15
2.5	Basic circuit of summing amplifier with two inputs. The output is the sum of the inputs but inverted due to inputs at negative terminal.	16
2.6	The schematic of summing amplifier used in the voltammetric system.	17

2.7	The schematic of the current to voltage converter. The triangular wave is applied to the carbon fiber electrode. The current from the carbon fiber electrode is converted into voltage by this circuit.	18
2.8	The voltage amplifier to amplify the signal to observe and process it on software. The amplifier has an adjustable gain, with the value of $R=10K\Omega$.	19
2.9	Data Acquisition Block	21
2.10	Front Panel of Data Acquisition Block	21
2.11	Filter Block	22
2.12	The voltammogram generator block	23
2.13	The graph generator block, generating cycle wise graph for the subtracted data	23
2.14	The data storage block	24
2.15	Stimulation electrodes made by two polyimide coated tungsten wire, separated from each other by 1 mm, the wires are then fixed parallel using 5-minute epoxy. one end should be peeled around $200\ \mu\text{m}$ while from the other side the coating is peeled till half the length.	25
2.16	The carbon fiber microsensor. Carbon fiber encased in polyimide coated fused silica capillary. The tip is sealed with biocompatible epoxy (<i>Epotek 301</i>). The thin capillary is supported by thick capillary using two component epoxy. On the other end carbon fiber is connected to metal connector using a silver adhesive	27
3.1	Voltammogram and dopamine concentration based on average of five recordings without stimulation and Pavlovian tasks.	32

3.2	Voltammogram and dopamine concentration when the stimulation electrode's dorso-ventral position was 7.4 mm. The black line below the voltammogram indicates the timing of stimulation.	33
3.3	Voltammogram and dopamine concentration when the stimulation electrode's dorso-ventral position was 7.5 mm (final depth). The black line below the voltammogram indicates the timing of stimulation.	34
3.4	Voltammogram and dopamine concentration (day1). Stimulation at 3 rd second. The timing of the stimulation is shown by a horizontal black line just below the voltammogram.	36
3.5	Voltammogram and dopamine concentration (day2). Stimulation at 3 rd second. The timing of the stimulation is shown by a horizontal black line just below the voltammogram.	36
3.6	Voltammogram and dopamine concentration (day3). Stimulation at 3 rd second. The timing of the stimulation is shown by a horizontal black line just below the voltammogram.	37
3.7	Voltammogram and dopamine concentration (day4). Stimulation at 3 rd second. The timing of the stimulation is shown by a horizontal black line just below the voltammogram.	37
3.8	The voltammogram and dopamine concentration recorded during presentation of unexpected primary reward (i.e. sucrose solution). Reward is presented at 3 rd second. Black arrow below the voltammogram shows the timing of the reward presentation.	39
3.9	The average voltammogram and dopamine concentration based on five trials with presentation of unexpected primary rewards (i.e. sucrose solution). Rewards are presented at 1 st second in all trials. Black arrow below voltammogram shows the timing of the reward presentation.	39

3.10	The voltammogram and dopamine concentration during presentation of a reward predictive stimulus (i.e. cue LED). The reward predictive stimulus was presented at 3 rd second of the recording. Black arrow below voltammogram shows the timing of the reward predictive stimulus.	40
3.11	The average voltammogram and dopamine concentration based on five trials with presentation reward predictive stimuli (i.e. cue LED). The reward predictive stimuli were presented at 1 st second in all trials. Black arrow below voltammogram shows the timing of the reward predictive stimuli in the trials.	41
A.1	Schematic of the amplifier circuit connected after headstage	55
A.2	Schematic of the pulse generator circuit	56
A.3	Schematic of the integrator circuit	57
A.4	PCB Layout of voltammetry System	58

List of Tables

2.1	Coordinates of carbon fiber, stimulation and reference electrodes .	29
3.1	Coordinates of carbon fiber and stimulation electrodes	33
3.2	Coordinates of carbon fiber and stimulation electrodes	35

Chapter 1

Introduction

Dopaminergic system and the effects of dopamine on various cognitive functions have attracted researchers since the advent of behavioural neuroscience few decades ago. Dopaminergic system, a region in the brain that comprises of the basal ganglia, secretes a neurotransmitter, dopamine which is of particular interest to neuroscientists due to its vast impact on various activities performed by the brain. Whether it is the movement or memory, reward or attention, learning or mood, many critical mechanisms are being regulated by this neurotransmitter.

Due to the importance of dopamine, scientists have devised various methods, invasive and non-invasive, for its detection. These methods include positron emission tomography (PET) imaging, high performance liquid chromatography (HPLC), microdialysis and voltammetry. PET and HPLC offer large scale monitoring but they come at the cost of less temporal resolution and slower processing. On the other hand voltammetry allows monitoring at a smaller scale with a higher temporal resolution.

Fast-scan cyclic voltammetry (FSCV) is the modified cyclic voltammetry with a high scan rate in the order of milliseconds, providing high temporal resolution.

This electrochemical technique can be useful in observing the mechanisms related to the release and re-uptake of the endogenous neurotransmitters (dopamine, in the present study).

The main emphasis of this thesis is the development of a practical, low-noise and low-cost system for voltammetric data acquisition and processing.

1.1 Dopamine and the Dopaminergic System

1.1.1 Dopamine

Have you ever thought about why people get addicted to drugs (Heroin and Cocaine)? Why diseases like Schizophrenia and Parkinson's occur? Why people get motivated in doing the work they like? And why they become less motivated to do the work they don't like? Why people like to use facebook? And why they learn something when reward or punishment is associated with it? All the answers lie in one word *dopamine*, a neurotransmitter from the family of catecholamines is released from the midbrain and is responsible for modulating reward and pleasure. It plays a viable role in behaviour and cognitive response including sleep, mood, learning, reward and motivation, it also has links with sociability [3],[4] and [5]. The results of various phylogenic studies indicate the presence of a relationship between dopamine and reward-related responses [6].

Dopamine has many functions, including effects in behavior and cognition, movement, attention, motivation and reward [7],[8], mood, sleep, and learning [9]. Its impact on motivation and learning is of particular note for decision making. It has also been linked with sociability and creativity.

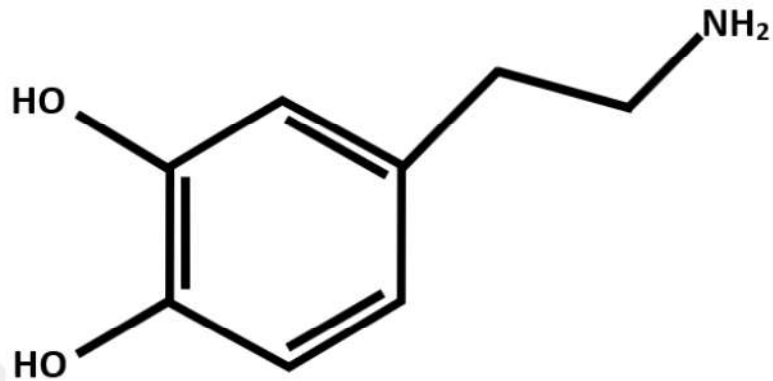


Figure 1.1: Molecular Structure of Dopamine [1]

The molecular structure of dopamine as shown in Figure 1.1 determines it as the member of catecholamine family. It is present in the body in its parent form that is *L-tyrosine* which undergoes hydroxylation and then decarboxylation to form *DOPAMINE*. These reactions take place in *Adrenal Medulla* [10],[11].

The Dopamine receptors can be pre-synaptic or both pre- and post-synaptic. The D_1 receptors are mostly post-synaptic while the others (i.e. D_2 , D_3 , and D_4) are both pre- and post-synaptic [12]. These receptors can be excitatory or inhibitory depending on the specific neuronal pathways [13].

1.1.2 Dopaminergic Pathways

The dopaminergic system consists of four main pathways, i.e. *nigro-striatal pathway*, *tuberoinfundibular pathway*, *mesolimbic pathway*, *mesocortical pathway*, as shown in the Figure 1.2.

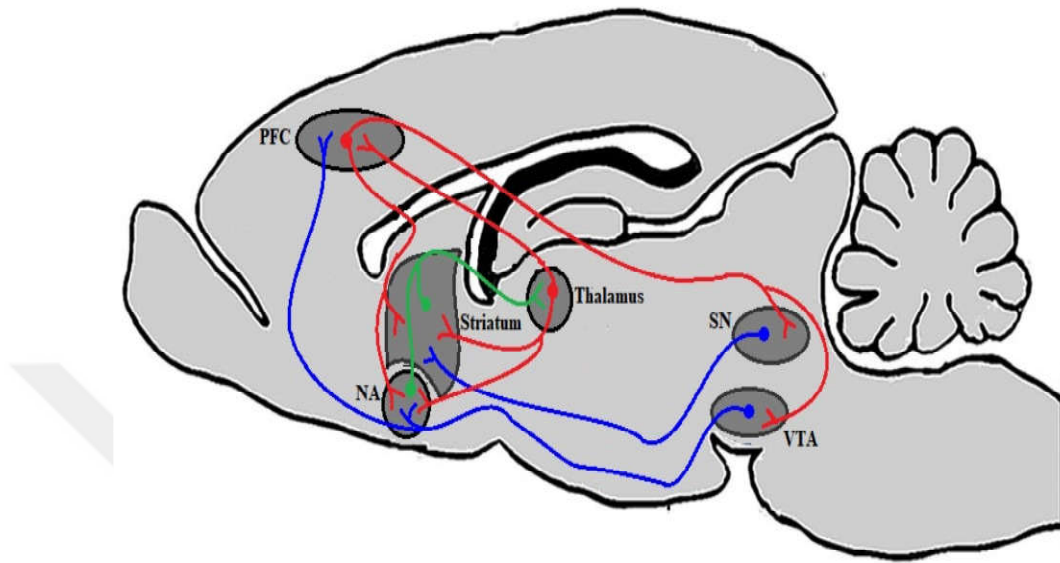


Figure 1.2: The dopaminergic pathways in the rat brain

The above mentioned pathways perform the following functions:

- **Nigrostriatal pathway:** This pathway is responsible for the movement behavior. The neurons of this region have their cell bodies in the substantia nigra and axon terminals in the dorsal striatum. The degeneration process of the neurons in this region results in the Parkinson's disease [14]. Further studies links these pathways with the feeding responses that is in reference to the reward aspects of the food and hunger regulation. [15],[16].
- **Tuberoinfundibular pathway:** This path regulates the secretion of prolactin from the anterior pituitary gland [17]. This pathway originates from the hypothalamus and the axon projections lie in the median eminence.
- **Mesocortical pathway:** The neurons of this pathway arise from ventral tegmental area and terminate at prefrontal cortex. This pathway is primarily associated with cognition and emotions. Schizophrenia is a type of mental disorder that is caused by excess dopamine in this pathway [18].
- **Mesolimbic pathway:** This pathway similar to the mesocortical pathway, originates from the ventral tegmental area (VTA) but has its projections to

the nucleus accumbens (NAc), a region in ventral striatum. It is related to the reward and pleasure behavior.

1.1.3 Physiology of the Dopaminergic System

Dopamine is a strong neurotransmitter that is responsible for various cognitive activities. Dopaminergic neurotransmission plays a vital role in the processing of reward related activities. In addition to controlling all motor and voluntary behavior, dopamine is also associated with certain hormonal secretions from the pituitary gland [19]. The release of dopamine is an indicator for some ongoing behavioral activities related with food thrive [20], reward based learning and goal mediated activities [7],[8]. Scientists have focussed their efforts on understanding the mesencephalic dopaminergic system to study motivation, controlled movements and reinforcement learning [21], [22].

The dopaminergic system has been divided into four main functional units. The region that is an efferent route between the substantia nigra and striatal region serves for the initiation and regulation of the motor circuits. Results of the experiments performed by Graybiel et al. suggests the that dorsal striatum is involved in the execution of controlled motor movements [23]. The degeneration of the neurons in the substantia nigra pars compacta projecting to the dorsal striatal region results in Parkinson's disease [24], and the hypokinesia due to this disease is the result of the dysfunctioning of neurons of nigrostriatal pathway [25]. Scientists observed the hypokinetic movements when they applied the lesion in nigrostriatal region of monkey's brain [26],[27].

The tuberoinfundibular pathway have the neurons based in hypothalamus and median eminence [28]. Results based on various tests claim the involvement of this region in functions of anterior pituitary gland [29]. Research also suggests the indirect involvement of the dopamine release in the median eminence in the release of Leutinizing Hormone (LH) [30].

The malfunction of mesocortical region, which is responsible for emotions and cognitive aspects of behavior, results in psychiatric disorders (Schizophrenia) and drug addiction [31], [32]. The effects generated by the dysfunction of mesocortical region results in the abberation of working memory and reward processing [33].

The fourth region of the dopaminergic pathway, the mesolimbic system is considered as the key region for processing reward related stimuli. The increased neuronal activity in the VTA results in the change of concentration of dopamine in nucleus accumbens (NAc) [34], [35]. Synaptic plasticity in this key region helps the animal in adaptating and performing reward related behaviors [36]. Schultz along with other researchers performed experiments on awake monkeys and observed the quick response of the mesolimbic neurons when reward stimuli is delivered [37]. Initially the neurons responds quickly with the availability of reward but after the extensive training the dopamine is observed to be released on the reward cue rather than the reward itself [9], [38]. The drug administration and addiction alters the release of dopamine in this region: the relation between the amount of cocaine administered and the released dopamine in NAc is studied and observed by Pettit and Justice [39]. Experiments based on supplying natural rewards resulted in the increased neuronal activity in the substantia nigra par compacta (SNc) in the monkeys brain [21] and higher dopamine secretion in the NAc of rat brain [20]. Cocaine blocks the dopamine transporters and in this way suppresses the reuptake of dopamine from the extracellular fluid [40].

1.2 Fast Scan Cyclic Voltammetry (FSCV)

1.2.1 Voltammetry

It is an electrochemical technique that is used to detect and measure the concentration of the neurochemicals present in a particular region. It is able to detect the neurotransmitters that are oxidizable such as catecholamines (dopamine, epinephrine and norepinephrine) and serotonin. In this method a particular current waveform with a certain voltage is applied on the electrode, usually carbon fiber. Due to the applied current waveform the neurochemical at the surface of the electrode oxidizes giving the current proportional to the concentration of dopamine. Since this mechanism depends on the phasic oxidization of neurochemicals, it makes it possible to measure the concentration in small timescale. Jaroslav Heyrovsky in 1959, got his nobel prize for his work on developing this technique. There are two main types of voltammetric methods. One is *cyclic voltammetry* in which a bipolar voltage waveform is applied as a function of time at constant current. The changing voltage waveform oxidizes the neurotransmitters which are in contact with the electrode. The other type of voltammetry is the *amperometry*. Unlike cyclic voltammetry, the amperometric method detects the chemicals at constant voltages. This method gives more accurate concentration values as compared to the cyclic voltammetry but unlike cyclic voltammetry it is not possible to distinguish the detected transmitter.

The main advantage of the voltammetric methods over other methods (e.g. microdialysis) is that it has great spatial resolution due to the small size of electrodes and better temporal resolution i.e. in the order of milli-seconds as opposed to minutes for the case of microdialysis. Since this work is based on cyclic voltammetry (more specifically FSCV), therefore we will discuss it further in the following section.

1.2.2 Fast Scan Cyclic Voltammetry (FSCV)

Fast scan cyclic voltammetry, as the name explains, is a faster implementation of the classically popular cyclic voltammetry technique to be used in reportedly fast manner, in every 100 ms. This technique was developed by London based scientist, Julian Miller in 1980s and has been frequently used for detection of one of the catecholamine, dopamine. As shown in the Figure 1.3, the substrate of the electrode that is used for FSCV is commonly carbon fiber, due to its advantage of providing a relatively wider voltage range as compared to the other substrates.

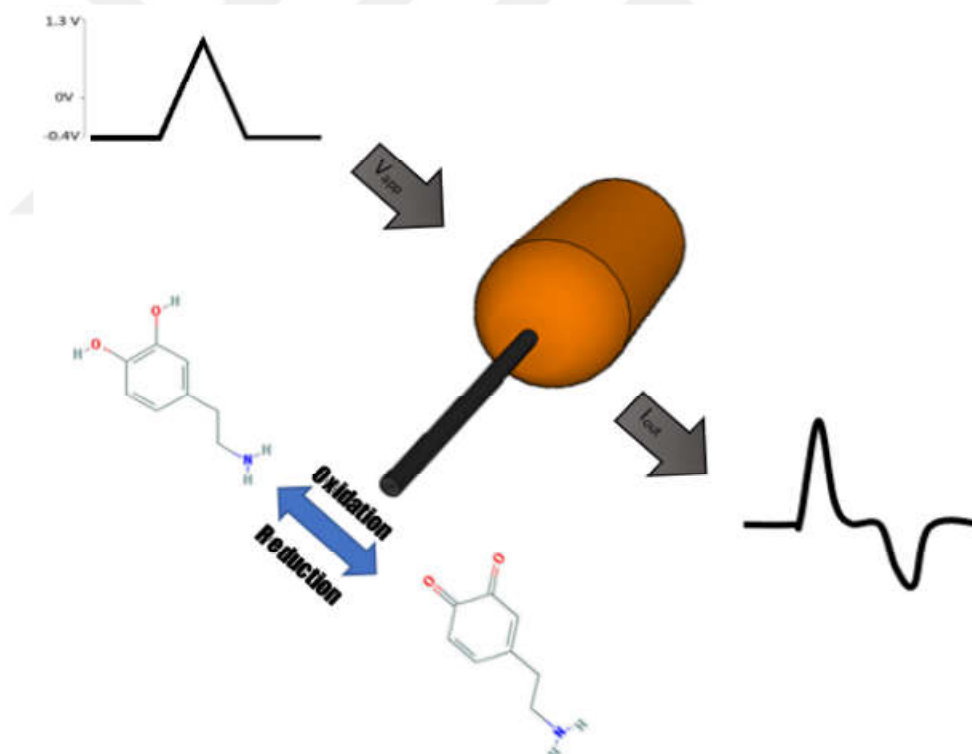


Figure 1.3: The principle of fast scan cyclic voltammetry

In this technique, the voltage is first kept at electrically idle state (-0.3 to -0.4 V) so that the neurotransmitter remains electrically neutralized, the voltage is then increased with a ramp at the rate of 300-400 V/s upto 1.3 V, and then decreased with the same rate back to -0.4 or -0.3 V. Dopamine gets oxidized during the positive increase in the waveform and becomes dopamine-o-quinone with the release of electrons. These electrons create current that is directly proportional to the molecules being oxidized at the surface of the electrode. This current is converted into voltage using current to voltage converter which gives the concentration peak indicating the amount of dopamine released. Since the waveform is bipolar, the oxidized dopamine-o-quinone is again reduced to dopamine in the negative phase of the waveform, giving the depression in the graph at around -0.3 volts. The data plotted against the voltage levels of the waveform is known as voltammogram that gives the clear representation of the species either dopamine or other amines that are oxidized and reduced. For the concentration profile, the peak value of oxidization level is plotted with respect to the scans giving the quantified concentration data of the whole scan period. In this work we have developed such system in our lab to successfully measure the release of dopamine in awake, freely moving chronically implanted rats.

1.2.3 Literature Review

Fast scan cyclic voltammetry is a robust technique for the detection of electroactive neurochemicals. Since its development, it has been widely used by the scientists worldwide. This method was developed by Julian Miller and associates about three decades ago [41], [42]. Initially it was considered to be able to detect only bio-amines, but with the recent developments in the system, pH [43] and various materials like serotonin [44], norepinephrine [45] and other chemicals can also be detected by this powerful tool. Among its various advantages are subsecond time resolution, sensitivity, some selectivity and great spatial resolution [16]. The method detects the electrical changes in extracellular fluid and traditionally uses insulated metal wires or carbon fiber encapsulated in glass capillaries [46].

FSCV is able to detect different groups at different voltage levels. Studies suggest that with this method different molecules like dopamine, serotonin, ascorbic acid and pH have different oxidation and reduction characteristics in cyclic voltammogram [47]. Dopamine which is the main catecholamine in this work oxidized at around 0.6 V while it reduces at -0.2 V [48]. This technique is capable of detecting rapid chemical reactions including the rapid detection of electroactive reactions [49] [50] [51]. An advantage of using FSCV is that it requires the use of very thin and small probes that gives minimal damage to the brain which is not even visible by light microscope [52].

As this is an electrochemical method, there are some issues related with the sensitivity. The first issue among those is the length of the carbon fiber that will face the adsorption process, the increase in length increases the number of sites being scanned [53]. Other problems associated with this technique are related to the scanning conditions and the nature of implant being acute or chronic. The pretreatment of electrode or the increased scanned potentials can increase the intensity of the signal but on the other hand decrease temporal resolution [54], [55] as these treatments alter the surface properties of the electrode. The sensitivity can also be decreased in chronic implantations. Gliosis is the reason behind it as the animal needs to recover after the surgery before any experiments are performed. The gliosis results in slower time response and decreased sensitivity as compared to the calibration data [56].

A major advantage of FSCV is its chemical selectivity. The selectivity of the system depends on the waveform applied as the oxidizing potentials of different chemicals varies. For example nitric oxide oxidizes at a much higher voltage potential than dopamine and other chemicals [57]. Although it is a powerful tool, FSCV is sometimes unable to distinguish between some electroactive compounds, for example dopamine and norepinephrine have nearly identical voltammograms due to the presence of same oxidizing hydroxyl group [47]. The main interferent that acts as a noise and suppresses the dopamine signal is the pH. This is the problem of any technique that involves the background subtraction [58], [59], but

this effect can be subtracted out as the pH signal is widely spread in each cycle as compare to the dopamine signal [48].

1.3 Objective of Thesis

Keeping in view the significance of dopamine in various behavioural and learning activities, and the importance of fast scan cyclic voltammetry in the detection of dopamine for in-vivo studies, this thesis focuses on design and implementation of a practical and low-cost voltammetry recording system.

The in-vivo detection of the changes in the physiological concentrations of dopamine presents challenges in hardware and software implementation since the dopamine related voltammetric current changes during behavioral experiments are around a few nanoamperes. In this context, our goal in the present study was to design, implement and integrate various hardware and software technologies to propose a fast scan cyclic voltammetry system which enables the monitoring of dopamine changes in the brains of behaving rats chronically implanted with carbon fiber microsensors.

Chapter 2

Methods

2.1 The Fast Scan Cyclic Voltammetry System

This section describes both the hardware and software aspects of the proposed voltammetry system. It also covers the acquisition parameters and characteristics of the wave generated by the voltammetry system.

2.1.1 Hardware

The high level block diagram of the hardware setup is shown in Figure 2.1. The main blocks of the system are voltammetric signal generator, the current to voltage converter and data acquisition (DAQ) system which will be described further in the following subsections.

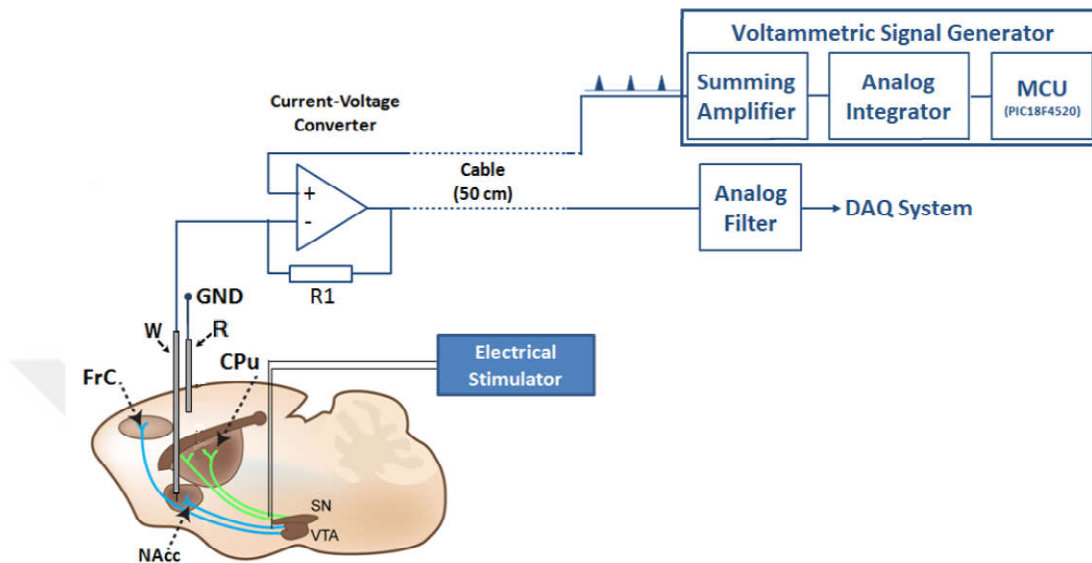


Figure 2.1: Basic structure of voltammetric hardware (modified from [2]).

2.1.1.1 Voltammetric Signal Generator

The purpose of voltammetry system is to generate a triangular wave at 10 Hz with a potential difference of 1.7 volts (i.e. -0.4V to +1.3 V) having the duration of 8.5ms. The waveform with these parameters are being widely used by the researchers to increase the sensitivity for in-vivo studies [60], [61]. The generation of this waveform requires a constant pulse generator, an integrator and a summing amplifier as shown in Figure 2.2.

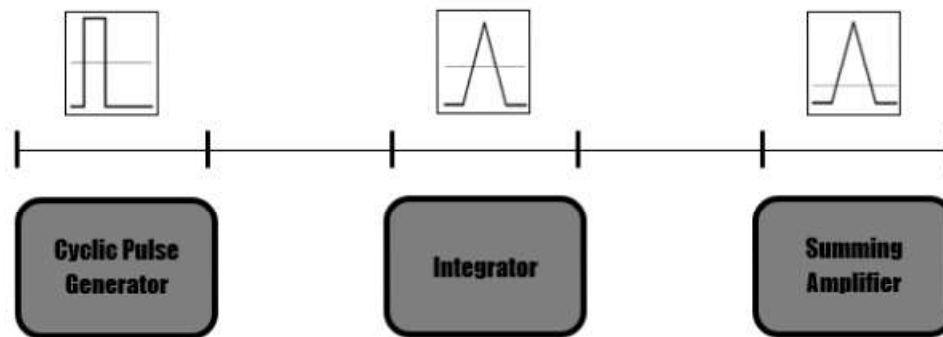


Figure 2.2: The block diagram of voltammetric signal generator

- Cyclic Pulse Generator:** The pulse generation operation is performed using *PIC18f4520* (a microcontroller from Microchip Technology). The code makes use of interrupts to generate pulses with a duration of 8.7 ms. The circuit uses 50 Hz main line synchronizer to align the timings of pulse generation and data acquisition, so that the interference from the mains line can be eliminated by subtraction during analysis of the needed data.

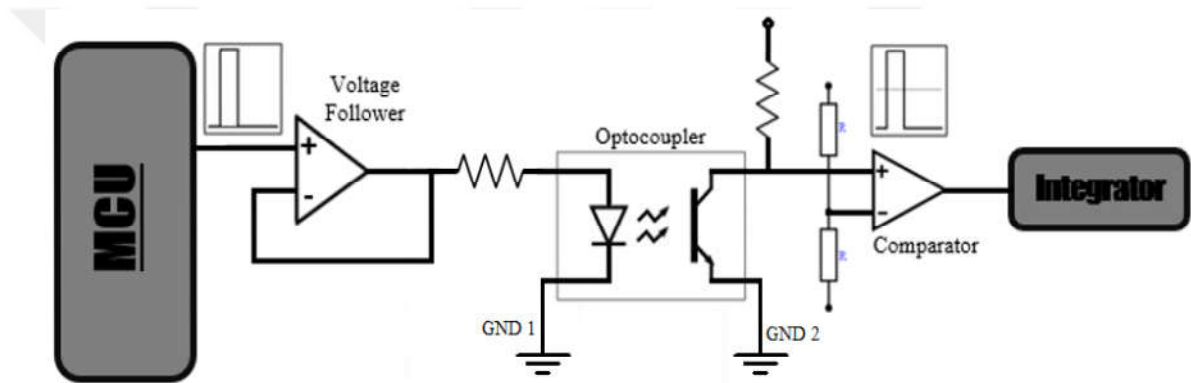


Figure 2.3: Architecture of pulse generator block. Microcontroller generates unipolar pulse signal which is first isolated using optocoupler and then converted to bipolar pulse signal using analog comparator.

Since the microcontroller works on 5 volts DC, it generates the pulses having only positive polarity. In order to solve this issue an analog comparator, *LM311* (Texas Instruments), is used. The comparator uses positive and negative voltage sources to convert the pulses into bipolar pulses. An issue faced during this step was the presence of noise in the pulse due to the clock frequency of oscillator. To resolve that issue, optocoupler (*4n25*) has been used with support of an op-amp (*MCP601*) in voltage follower configuration before the comparator. This architecture is shown in Figure 2.3.

- The Integrator:** Integrator is required to generate a triangle wave by performing integration of the square wave. It involves using operational amplifier (*MCP-601*) in integrator configuration. The basic reason of using *MCP-601* (Microchip Technologies) is its rail to rail operation that allows the use of whole supply voltage range in its operations. The integrator is

an RC circuit that makes the use of values of resistance and capacitance to control the rate of change in output voltages. Figure 2.4 represents the circuit diagram of op-amp based integrator.

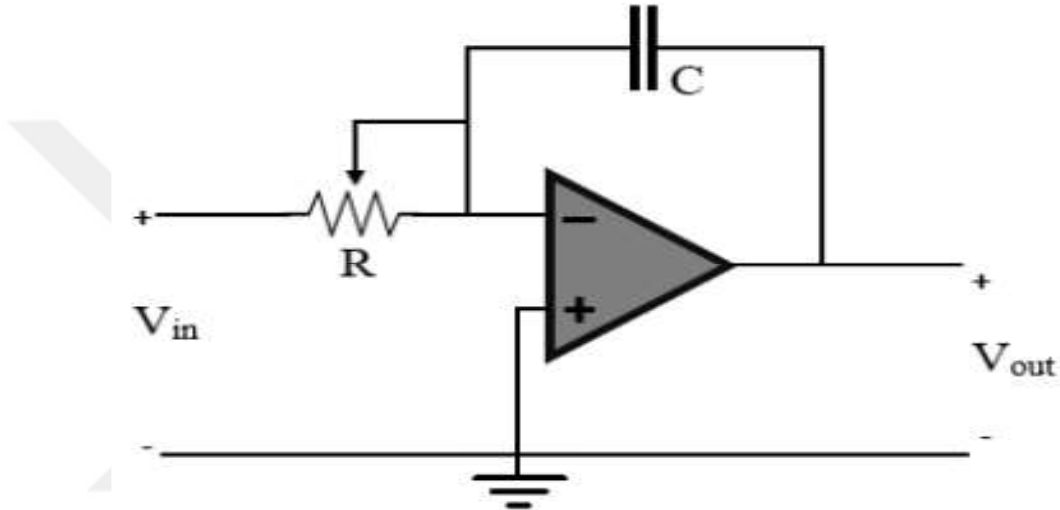


Figure 2.4: The integrator circuit with constant capacitance and variable resistor. The resistance can be used to control the ramp of the triangular waveform.

Since the time period of the triangular wave is controlled by adjusting the pulse width, the only way to control the ramp of the triangle is either controlling the values of resistance or capacitance. The output of an integrator can be calculated by the following equation:

$$V_{OUT} = -\frac{1}{R_{in}C} \int_0^t V_{IN} dt \quad (2.1)$$

The simplified version of Equation 2.1 can be written as:

$$V_{OUT} = -\frac{1}{j\Omega R_{in}C} V_{IN} \quad (2.2)$$

where C is the feedback capacitance and R is the variable input resistance. The negative sign indicates the 180° phase change in the output which is due to the input on negative terminal. We have used $1 \mu\text{F}$ and using Equation 2.1, the value of R is set to be around $4.8 \text{ k}\Omega$.

- Summing Amplifier:** The summing amplifier is used to adjust the amplitude and offset of the generated triangular wave. It is an application of operational amplifier that is used to combine multiple input voltages into single output. Figure 2.5 shows a basic summing amplifier circuit. The configuration with all the input resistance of similar values is known as *voltage adder*. If the values of all input resistance are not same then this configuration is also known as *scaling summing amplifier*. In our experiment, we use the latter configuration.

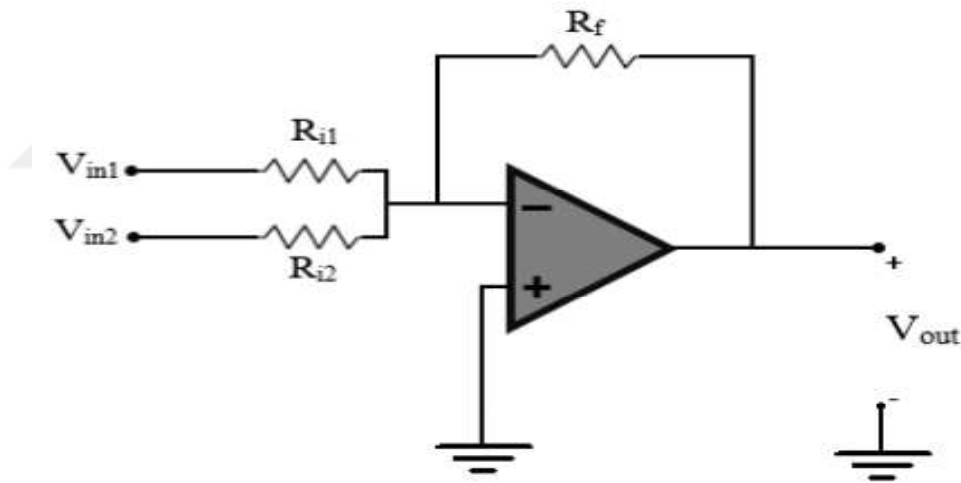


Figure 2.5: Basic circuit of summing amplifier with two inputs. The output is the sum of the inputs but inverted due to inputs at negative terminal.

The equations of the output voltages in both adder (Equation 2.3) and scaling (Equation 2.4) configuration are given below:

$$V_{OUT} = -\frac{R_f}{R_i}(V_{in1} + V_{in2} + \dots) \quad (2.3)$$

$$V_{OUT} = -R_f\left(\frac{V_{in1}}{R_{i1}} + \frac{V_{in2}}{R_{i2}} + \dots\right) \quad (2.4)$$

The purpose of using summing amplifier here in scaling configuration is to adjust the amplitude of generated triangular wave and to set its offset so

that the wave lie between -0.4 to +1.3 V. The IC used for this circuit is same as the previous circuit (MCP-601). The schematic of the summing amplifier as used in our experiment is shown in Figure 2.6.

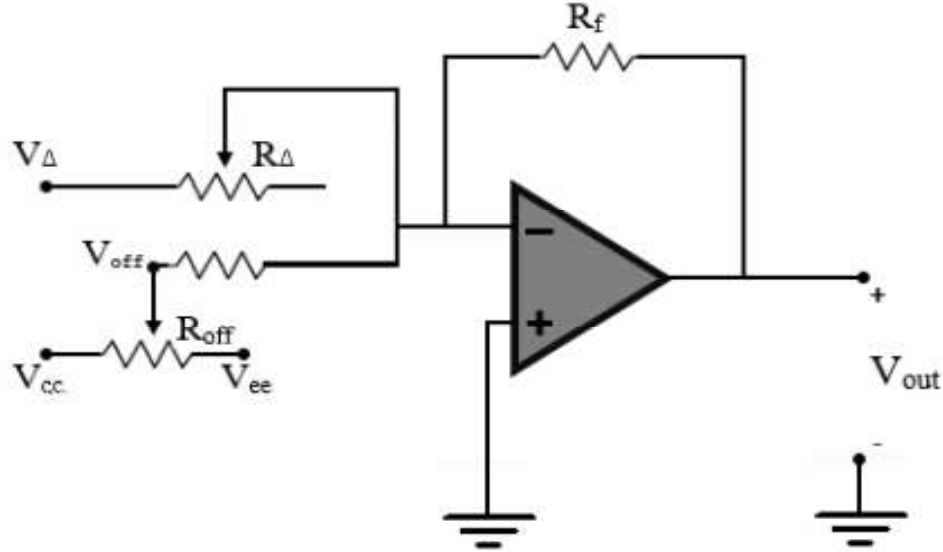


Figure 2.6: The schematic of summing amplifier used in the voltammetric system.

In Figure 2.6, V_{Δ} is the input from the integrator while the the V_{off} is the input for offset adjustments. R_{Δ} controls the amplitude of the triangular wave while R_{off} is responsible for setting the offset. The V_{out} equation for this formation is given as follows:

$$V_{OUT} = -R_f \left(\frac{V_{\Delta}}{R_{\Delta}} + \frac{V_{off}}{R_{off}} \right) \quad (2.5)$$

2.1.1.2 Current to Voltage Converter

As the name indicates, this op-amp based circuit is used to convert the current that appears due to oxidation of dopamine into proportional voltages. The circuit is placed on the head stage that can be connected to the animal. Since the headstage should be light and small, *OPA2604* from Texas Instrument is used in SMD packaging. The circuit formation that has been used in our system is

shown below.

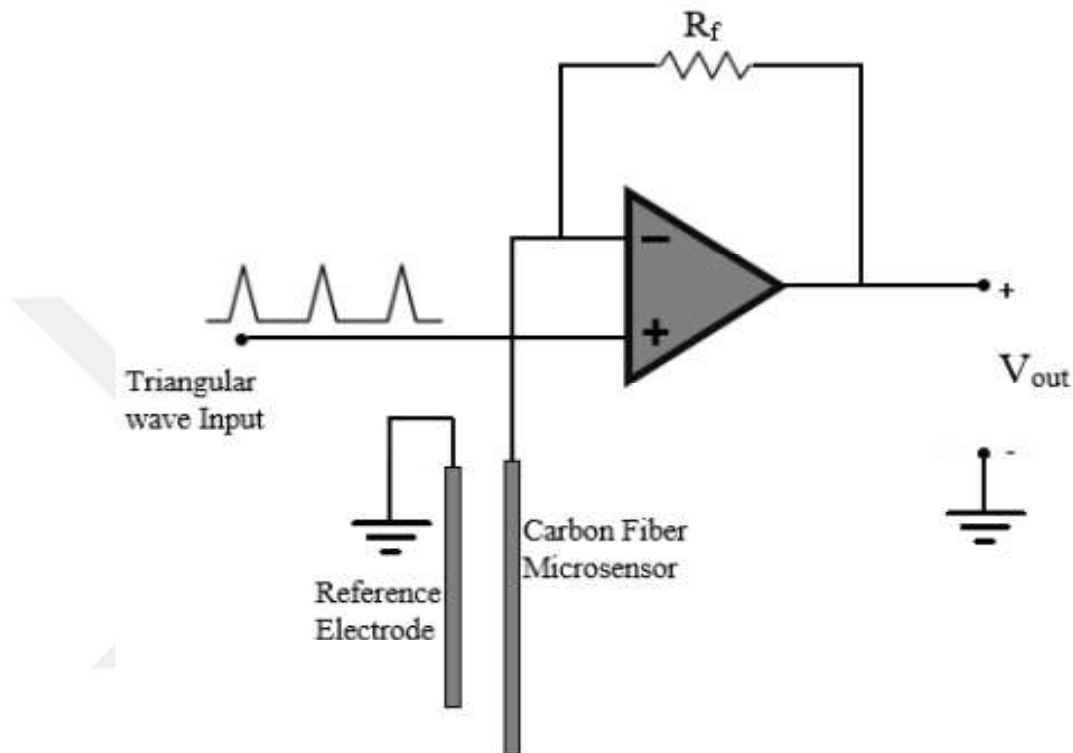


Figure 2.7: The schematic of the current to voltage converter. The triangular wave is applied to the carbon fiber electrode. The current from the carbon fiber electrode is converted into voltage by this circuit.

The circuit shown in Figure 2.7 converts the current from the carbon fiber electrode into voltages. The feedback resistance used here is $1\text{ M}\Omega$. The output of this converter is followed by a low pass filter.

Output of the low pass filter is fed to a signal amplifier with adjustable amplification as shown in Figure 2.8. The resistors used here are of equal values.

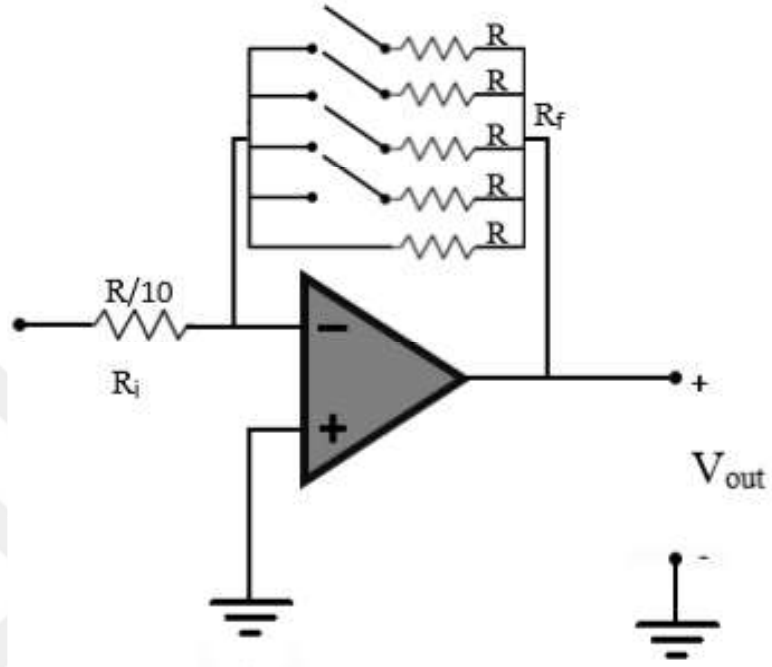


Figure 2.8: The voltage amplifier to amplify the signal to observe and process it on software. The amplifier has an adjustable gain, with the value of $R=10K\Omega$.

With every resistor applied, the gain is decreased. The current detected by the electrode can be calculated by the following equation:

$$I_{OUT} = -\frac{V_{OUT}}{R_{cf}} \times R_i \times \left(\frac{1}{R_f} + \frac{1}{R_{f1}} + \frac{1}{R_{f2}} + \dots + \frac{1}{R_{fn}} \right) \quad (2.6)$$

where V_{OUT} is the output of the amplifier, R_f and R_{fn} are the feedback resistors of the amplifier, R_i is the input resistor of the amplifier. R_{cf} is the feedback resistor of current to voltage converter circuit. By using the values of resistances as shown in Figure 2.8 and the value of R_{cf} to be $1 \text{ M}\Omega$. Equation 2.6 can be simplified into the following equation:

$$I_{OUT} = -\frac{V_{OUT} \times (n + 1)}{10^6 \times 10} \quad (2.7)$$

where n in this equation is the number of extra resistors connected other than the main resistor as shown in Figure 2.8.

2.1.1.3 Data Acquisition System

The analog signal is then converted into digital signal for data storage, baseline subtraction and other processing. The output of the voltage converter is fed to enter data acquisition board. It is a 12 bit data acquisition board with PCI interface (*National Instruments*, NI PCI6040E). Two analog input channels (AI-0 and AI-1) have been used in this setup, one for the acquisition of data and the other to trigger the acquisition. Further channels can also be used depending on the requirement or the number of inputs that needs to be acquired. The computer used for this application has a Core I5 (Intel Corporation) processor (dual core) with the processing speed of 3.20 GHz and 12 GB RAM.

2.1.2 The Software

The acquisition and processing of the voltammetric signals is performed on Labview (National Instruments) based customizable system. The basic software consists of various modules that are combined together to perform acquisition, filtering, subtraction, display and storage. These modules are described one by one as follows:

2.1.2.1 The Acquisition Block

This module is responsible for acquiring the signals in each cycle and concatenating the data into an array for further use. This acquisition is done using DAQ assist VI, that gets the data after receiving an external trigger. It acquires 3000 samples at the rate of 200 kHz. The acquisition time can be adjusted to automatically terminate the process after acquiring the required number of samples and concatenating them into an array for further processing. This block contains the cues for the acquisition status and reward time. The block diagram and GUI front

panel of the acquisition block are show in Figure 2.9 and Figure 2.10, respectively.

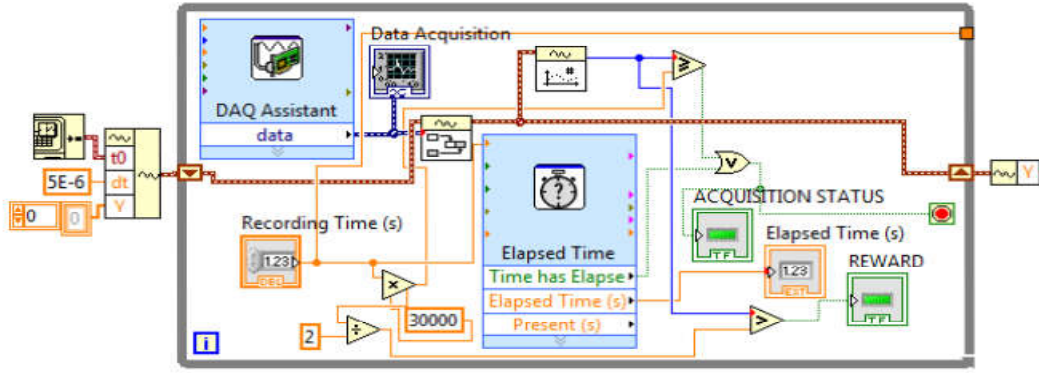


Figure 2.9: Data Acquisition Block

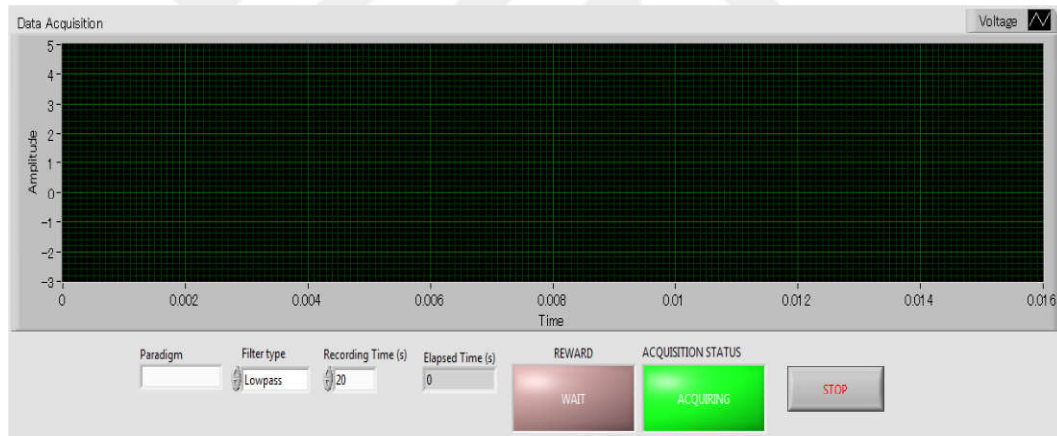


Figure 2.10: Front Panel of Data Acquisition Block

The first half of the data array contains baseline signal while the latter half comprises of reward delivery signal. All the baseline signals are added and then averaged to give a better signal as a baseline for subtraction.

2.1.2.2 The Filter Block

The filter block contains a low pass filter that filters the data in the array before subtraction. This block attenuates the frequencies above 1 KHz (with the sampling frequency of 200 KHz). The order of the filter is set to be 4. The labview block of low pass filter is given in Figure 2.11.

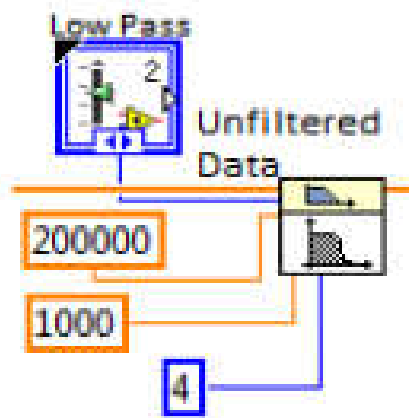


Figure 2.11: Filter Block

2.1.2.3 The Subtraction Block

The subtraction block subtracts the baseline signal from the signal we are interested in. The baseline signal here corresponds to the average of the hundred cycles acquired just before the starting of the signal we are interested in. The baseline average signal is then subtracted from each cycle of the reward signal. The cycle number serves as input to the subtraction block which extracts the baseline and reward signal corresponding to the cycle number. This block is based on loop based programming so it performs the subtraction on all the cycles sequentially. The above defined process is applied on both filtered (output from the filter block) and unfiltered (raw) signal before displaying the resultant signal on waveform graph monitor.

2.1.2.4 Display and storage block

After subtraction, the data is displayed and also stored for later use. The data from the array is segmented into cycles and displayed in the form of graph or voltammogram. The block diagram of display and storage block is shown in Figure 2.12 and Figure 2.13 respectively. The graph can be seen for each cycle while the Voltammogram represents cycles or time on x axis and voltage levels

on y axis. The color scheme of the voltammogram is also adjustable. The output results of voltammogram and the graph monitor are shown in chapter 3.

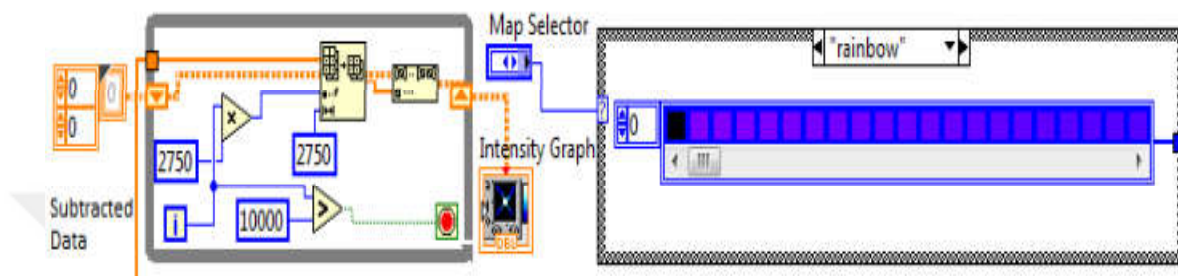


Figure 2.12: The voltammogram generator block

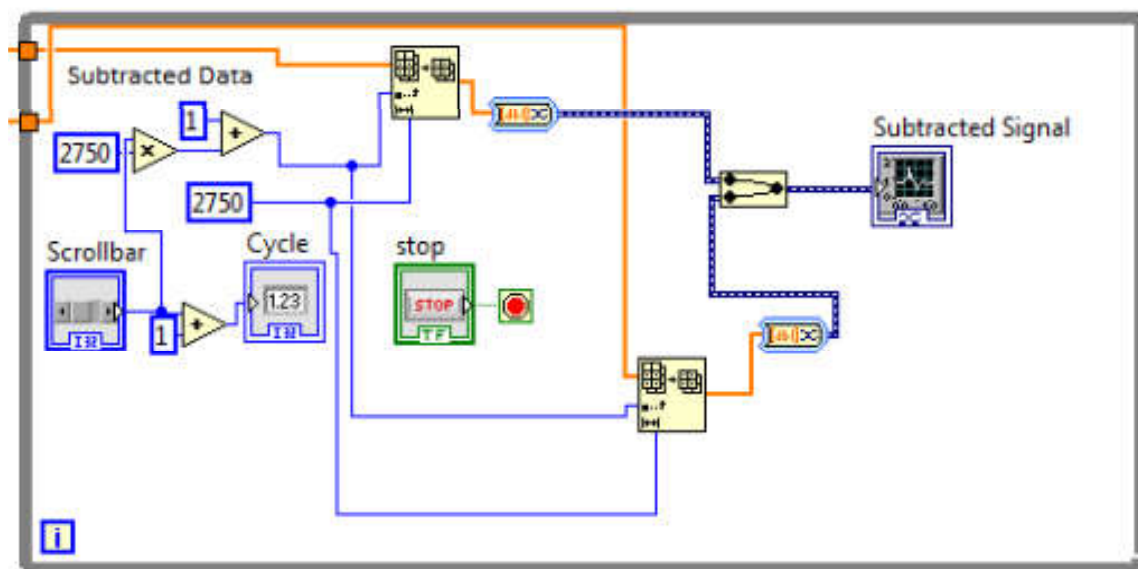


Figure 2.13: The graph generator block, generating cycle wise graph for the subtracted data

The processed data is also stored in an excel file (.csv). The files are stored in the specific paradigm folders. The file is named automatically according to the time of experiment.

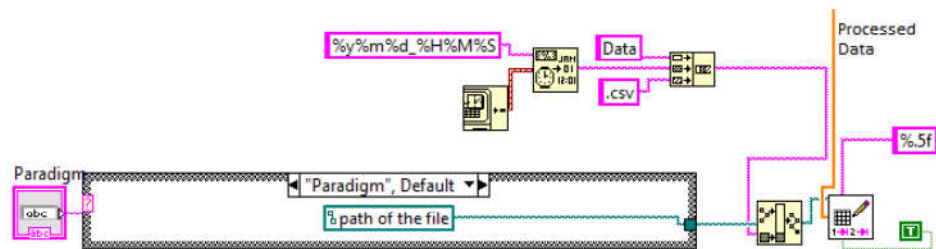


Figure 2.14: The data storage block

The basic voltammetry software is concluded here. There are some customizable features that can be added in the program such as saving the timestamps of the activities (cues) during experimentations and external triggering of other hardware to synchronize the activities with acquisition.

2.2 The Microsensors, The Reference and Stimulation Electrodes

This section will cover the preparation methods for stimulation electrodes, reference electrodes and carbon fiber microsensors.

2.2.1 Reference Electrodes

In this study, Ag/AgCl electrodes have been used. These electrodes are prepared by using silver wire of 0.2 mm diameter (Warner instruments). The wire is coated with chloride ions by the process of electroplating. This is done using stainless steel wire as cathode and silver itself as anode. Both the wires are then submerged in HCl solution for 2-3 minutes or till the area of the silver electrodes that is submerged becomes grey. The color is due to the oxidation of chlorine on the surface of silver electrode. The Ag/AgCl electrode then becomes ready to be

used for implantation.

2.2.2 Stimulation Electrodes

The electrodes for stimulating the dopaminergic pathways consist of two straight tungsten wires (0.005 inch diameter) coated with polyimide (Plastics One, 005TW/30S). The ends of the wires should be blunt and not sharp to reduce injury impact on brain tissue. Both the filaments are peeled from one side using a blade. The peeled off region of both the filaments should be equal and around $200\ \mu\text{m}$ in length. On the other side the coating can be peeled of around 1 cm to connect the tungsten wires to the electrical stimulation device.

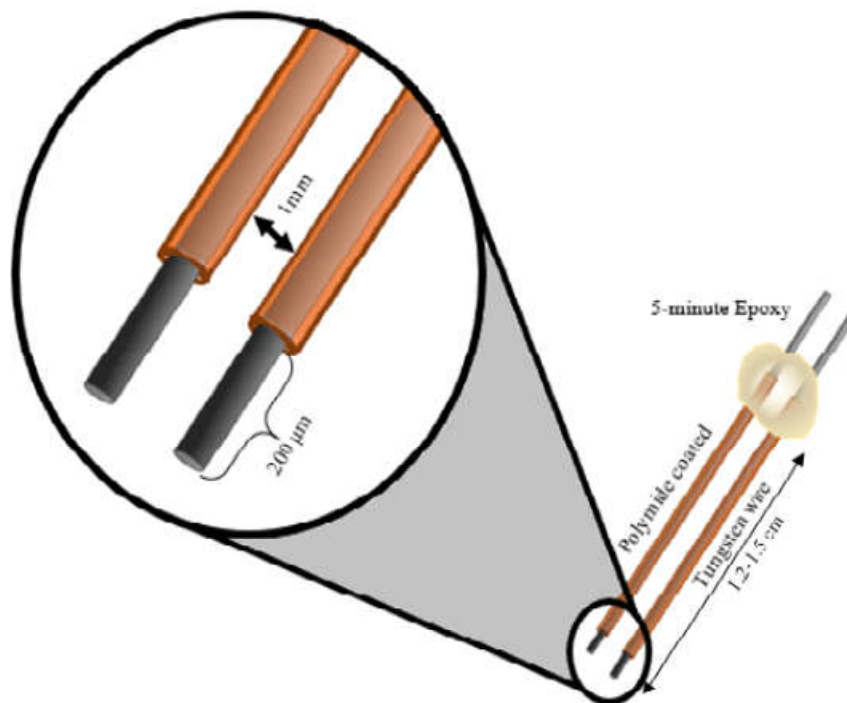


Figure 2.15: Stimulation electrodes made by two polyimide coated tungsten wire, separated from each other by 1 mm, the wires are then fixed parallel using 5-minute epoxy. one end should be peeled around $200\ \mu\text{m}$ while from the other side the coating is peeled till half the length.

Both wires are then carefully arranged parallel to each other at a distance of 1 mm. The position of the filaments with respect to each other are then fixed using two component epoxy. After getting cured, these electrodes are ready to be implanted as well.

2.2.3 Carbon Fiber Microsensor

The microsensor for dopamine detection is composed of very thin fused-silica capillary and a carbon fiber passing through its lumen [62], [63]. This section describes the fabrication and calibration method for the carbon fiber electrode.

- **Fabrication:** The process starts when a single carbon fiber (Goodfellow Corporation, C005722) is pulled into Polymide coated fused silica capillary (Polymicro Technologies, TSP020090) using a vacuum pump. This process is carried out with the carbon fiber submerged in ethanol. The capillary, with outer diameter of 90 μm , is fixed and supported from one side with a wide capillary. The capillary is then allowed to dry for couple of hours. Afterwards, the tip of the capillary is sealed to fix the carbon fiber position.

The seal applied on the tip of the capillary is a two component bio-compatible epoxy (*Epotek, 301*). The epoxy should be viscous so that it becomes a smooth bulb like structure at the surface as shown in Figure 2.16. The shape of the tip should be as smooth as possible to avoid or reduce tissue damage during implantation. The electrode is then left to cure the epoxy at the tip for a day.

After curing, metal contact is attached to the capillary. This contact provides support to the capillary and gives the medium of connection to the carbon fiber. A silver adhesive (Loctite Corporation, MR 3863) is applied to connect the carbon fiber and the metal contact and is allowed to be

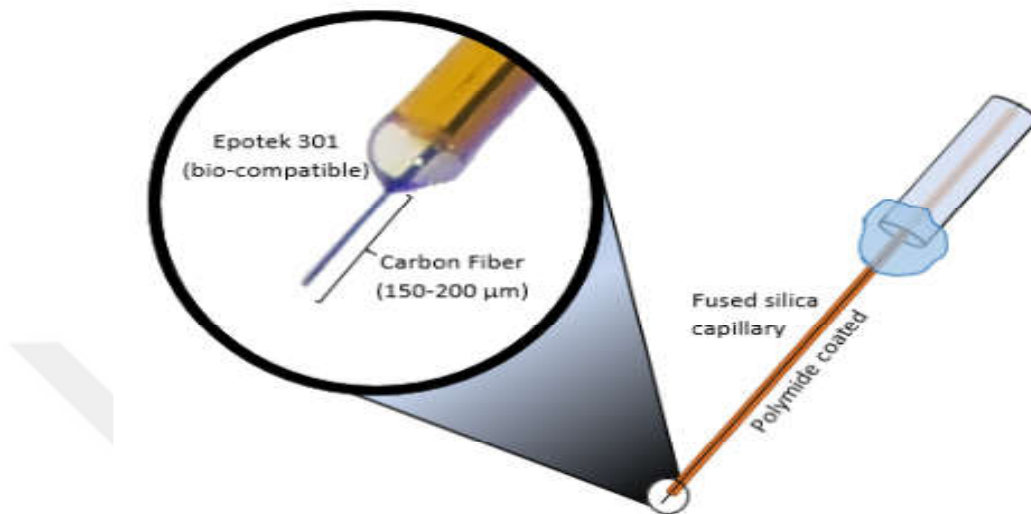


Figure 2.16: The carbon fiber microsensor. Carbon fiber encased in polyimide coated fused silica capillary. The tip is sealed with biocompatible epoxy (*Epotek 301*). The thin capillary is supported by thick capillary using two component epoxy. On the other end carbon fiber is connected to metal connector using a silver adhesive

cured. The connection between the capillary and metal contact is further strengthened by sealing the connecting point with dental acrylate. At the end, the protruding fiber from the sealed end is trimmed to 150-200 μm [64]. The electrode at this stage is now ready for calibration and implantation.

- **Calibration:** This process uses a Matlab (Mathworks Inc.) program developed by the author. The program acquires a 10-seconds sequence of data for both baseline and dopamine signals. The dopamine data sequence is then subtracted from the baseline signal to obtain the concentration in the form of voltage. The carbon fiber and reference electrodes are submerged in saline (0.9% isotonic solution) till the carbon fiber electrode is stabilized (neutralized subtracted data). After the electrode is stabilized, the program takes one baseline recording. 1 μM dopamine is then added to the saline solution.

New dopamine recordings are then acquired and subtracted from the pre-acquired baseline. The subtracted data is then plotted on graph that gives

the voltage values proportional to the concentration of dopamine being oxidized. The data acquisition for the dopamine signal goes on until the subtracted signal is stabilized or stops increasing. This value is considered as the highest sensitivity of the electrode which is then converted into current values per μM dopamine solution by using Equation 2.7. The electrodes with highest sensitivities and good physical conditions are selected for implantation.

2.3 Surgical Procedure

The apparatus that is used in the surgery is sterilized beforehand. Male rats (Sprague Dawley) weighing between 300 to 400 grams and aged between 3 to 6 months are selected for implantation. The rats are first anesthetized with ketasol (57 mg/kg) and xylazine(5.7 mg/kg). After the rats are completely anesthetized (approximately 10 minutes) they are fixed to the stereotaxic frame. The hair on the head are shaved and a vertical incision is made on the skin. After holding the skin using speculum, the muscle layer is also removed to access the cranium. Perhidrol is applied on the skull to clean the tissue residue on the bone and bregma is marked. The position of the carbon fiber, stimulation and reference electrodes are marked onto the skull with reference to the bregma. The coordinates of the electrodes are given in the Table 2.1. Four screws are then inserted in the skull to anchor the headstage. The screws must be tight and there shouldn't be any leakage of cerebrospinal fluid (CSF). Thin layer of dental acrylate is applied on the junction between the screws and skull.

Craniotomy is created using drilling station (Dremel, model 3000). First the reference electrode is inserted slowly and fixed by dental acrylate. After fixing the reference electrode, the dura matter of both stimulation site and the CF electrode site are removed carefully without damaging the brain. After this, the carbon

	Carbon Fiber Electrodes	Stimulation Electrodes	Reference Electrodes
Anterior/ Posterior (mm)	+1.5	-4.6	+2.5
Median/ Lateral (mm)	-2.1	-1.3	+2.5
Dorsal/ Ventral (mm)	6.4 to 7.2	7.4 to 8.4	3 to 3.5

Table 2.1: Coordinates of carbon fiber, stimulation and reference electrodes

fiber is lowered to the surface of brain till a slight change in the triangular waveform is observed. This vertical location is noted as the dorsal/ventral coordinate of the brain surface and the electrode is further lowered very slowly (with a rate of $50 \mu\text{m}$ a minute) using a micropositioner (Narshige, MO-82), till the target location. Same procedure is performed for the stimulation electrode followed by a waiting period till stabilization in the voltammetric signal is achieved. The recordings are then performed, electrodes are moved further till the optimum position of the electrodes (maximum dopamine level) can be found. The electrodes are then fixed with dental acrylate. Once the dental acrylate is cured, the connectors are fixed and surrounded by the same material to make a robust head stage.

The rat is then removed from the stereotaxic frame and is injected with intramuscular injection of Carprofen 7.4 mg/kg on the surgery day and the day after. The rat is then allowed to recover for one month after surgery before behavioral experiments can be performed.

2.4 Experiments

This section consists of the description of three different experimental paradigms regarding dopamine release. One of them is based on electrical stimulations of the dopaminergic pathway while the other two paradigms consider Pavlovian conditioning.

- **Stimulation Task:** In this task, the awake rat is stimulated by biphasic pulses. The stimulator provides constant current pulses with various configurations. The data is acquired using Labview program as discussed earlier and then the voltammogram is plotted to display the dopamine concentration change during electrical stimulation. The results are shown in Chapter 3.
- **Behavioral Task (*Pavlovian Conditioning*):** In behavioral experiments, the rat is kept thirsty for 24 hours and then the training is initiated. In first task, the rat is trained to anticipate the release of reward on hearing an audio cue, a click sound produced by solenoid valve. In the following task the rat is trained to get reward (sucrose solution) three seconds after the LED cue is turned ON. 0.2 mL of 13% Sucrose solution is delivered in each trial. It took around three days for each rat, with 100 trials per day to get trained. In other task, the rat is further trained to press the lever only when the LED cue is turned ON, this lever press initiates the reward delivery. These experiments are performed in the behavioral cage developed in the lab. The results of both paradigms are displayed in the results section of this study.

Chapter 3

Results

This section will demonstrate the practicality of the described voltammetry system with recordings from the rat chronically implanted with carbon fiber electrode. The results included are obtained from the recordings on freely moving rat when there is no any activity (either electrical stimulation or reward related activity), recordings during electrical stimulation of the dopaminergic pathway and from the recordings during behavioral experiments. The results are described as follows:

3.1 Voltammetric Recordings of Rat in Idle State

These recordings are made when the awake and freely moving animal (Rat-1) was not performing any task. In these recordings, the ten seconds (100 cycles) baseline signal is recorded prior to the main recording, the baseline signal is then averaged and used for subtraction from the main signal.

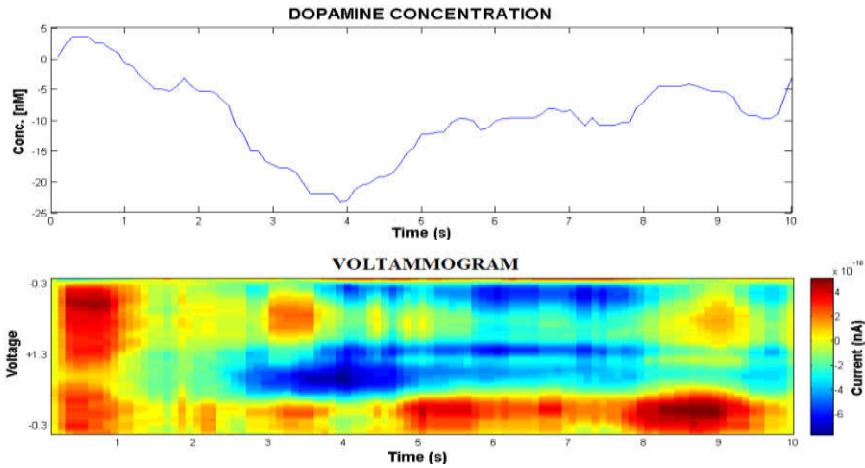


Figure 3.1: Voltammogram and dopamine concentration based on average of five recordings without stimulation and Pavlovian tasks.

The result shown above is the average of five recordings of 10 seconds from (Rat-1) in idle state (when there is no stimulation or reward related tasks). The average dopamine concentration from Figure 3.1 is measured to be $-9.45 \pm 6.58nM$. This concentration is the overall average of data based on 50 seconds recording .

3.2 Voltammetric Recordings During Stimulation of the Dopaminergic Pathway

This section covers the results of the recordings during the surgery and after recovery from the surgery with electrical stimulation of the dopaminergic pathway:

3.2.1 During Surgery

The experiments are realized with a Sprague Dawley rat (Rat-1), six months old and weighing around 340 grams. The rat was being implanted with a carbon fiber electrode in nucleus accumbens *NAcc* and stimulation electrode in median

forebrain bundle with coordinates in Table 3.1. There are two recording sessions, having different depths of stimulation electrodes. The stimulating pulses are applied at third second of each recording.

	Ant/Pos (mm)	Med/Lat (mm)	Dorso/Ven (mm)
Carbon Fiber	+1.5	+2.1	6.4
Stimulation	-4.6	+1.3	7.5

Table 3.1: Coordinates of carbon fiber and stimulation electrodes

The stimulation parameters are :

- Amplitude: $100 \mu\text{A}$.
- Frequency: 60 Hz.
- Pulses : 60 biphasic pulses.
- Pulse Duration : $2000 \mu\text{sec}$.

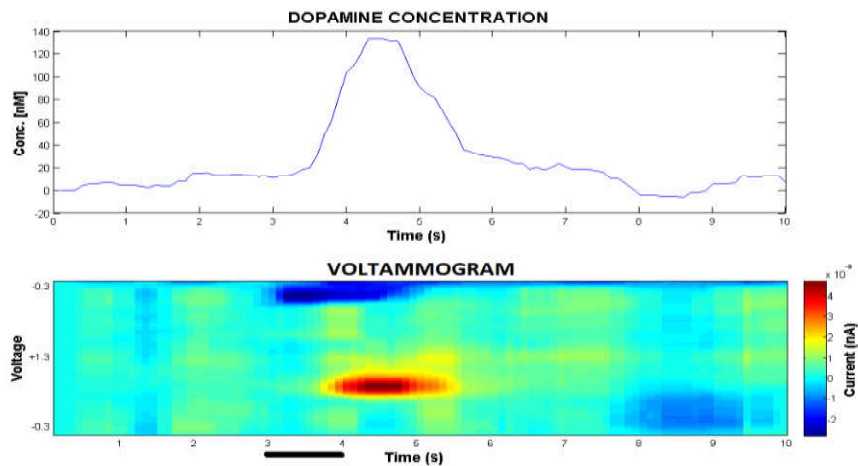


Figure 3.2: Voltammogram and dopamine concentration when the stimulation electrode's dorso-ventral position was 7.4 mm. The black line below the voltammogram indicates the timing of stimulation.

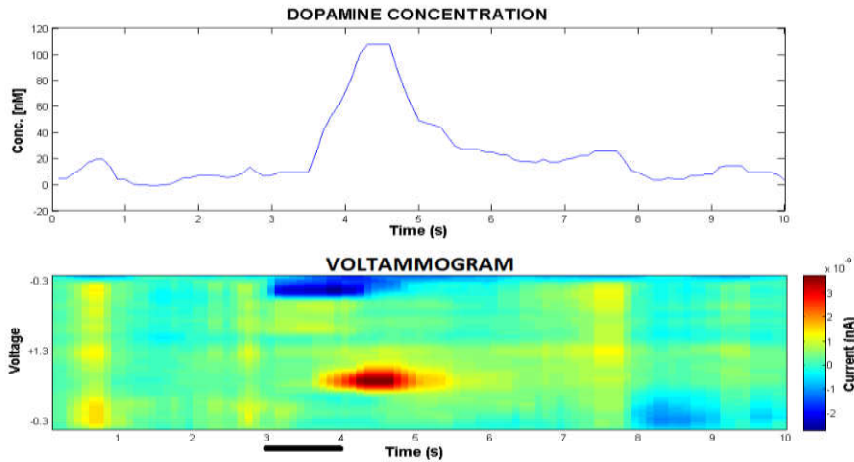


Figure 3.3: Voltammogram and dopamine concentration when the stimulation electrode's dorso-ventral position was 7.5 mm (final depth). The black line below the voltammogram indicates the timing of stimulation.

The results shown above demonstrates the successful working of voltammetric system, giving concentration of dopamine released. The recordings shown above are taken with the carbon fiber in nucleus accumbens at a fixed dorsoventral position of 6.4 mm, while searching for the depth of the stimulation electrode at which it can stimulate the maximum number of dopaminergic neuron resulting in the maximum detection of the dopamine concentration. In the above results, the stimulating pulses are applied at 3rd second. It is observed that the dopamine reaches the peak value just after stimulation ended that is 1 second after the initiation of the stimulating pulses. The reuptake time is observed to be around 1.25 seconds. The peak dopamine concentration at 7.4 mm dorsoventral position of the stimulating electrode is found to be 132.8nM whereas, at 7.5 mm depth the peak value detected was 106.9nM. The dopamine observed in the above results is in good concentration, but the damage to the neuronal tissue by electrode results in glial activity, that may result in the decrease in sensitivity of the electrode. In order to validate the system for smaller concentrations, we performed the stimulation experiments after recovery period (one month) and performed some behavioral experiments aswell. The results for the discussed experiments are discussed in further subsections.

3.2.2 After Recovery

The recordings shown in this part are realized with a Sprague Dawley rat (Rat-2), five and a half months old and weighing around 360 grams. The rat was implanted in nucleus accumbens *NAcc* and median forebrain bundle with coordinates shown in Table 3.2. All the results displayed below are based on recordings made during the electrical stimulation experiments performed after the recovery from the surgery. The recordings are performed at different days. The stimulating pulses are applied at third second of each recording.

	Ant/Pos (mm)	Med/Lat (mm)	Dorso/Ven (mm)
Carbon Fiber	+1.5	+2.1	7.0
Stimulation	-4.6	+1.3	8.9

Table 3.2: Coordinates of carbon fiber and stimulation electrodes

The stimulation parameters are:

- Amplitude: 100 μ A.
- Frequency: 60 Hz.
- Pulses : 60 biphasic pulses.
- Pulse duration : 2000 μ sec.

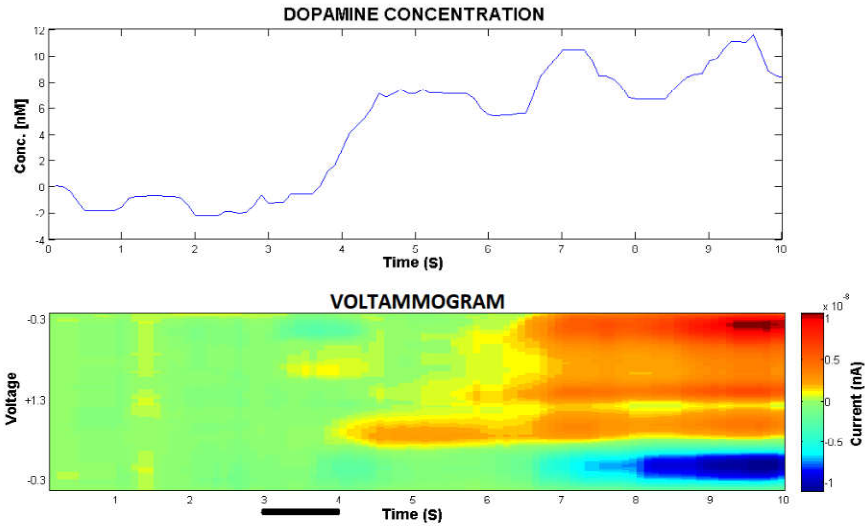


Figure 3.4: Voltammogram and dopamine concentration (day1). Stimulation at 3rd second. The timing of the stimulation is shown by a horizontal black line just below the voltammogram.

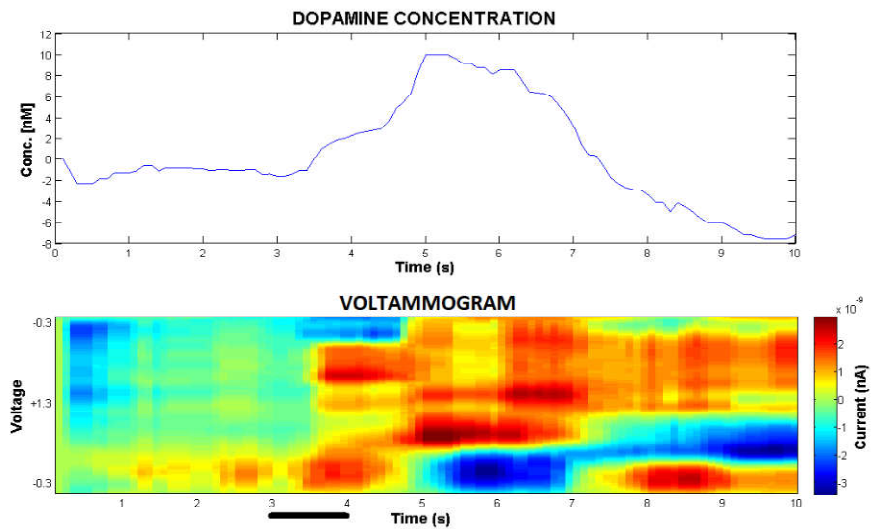


Figure 3.5: Voltammogram and dopamine concentration (day2). Stimulation at 3rd second. The timing of the stimulation is shown by a horizontal black line just below the voltammogram.

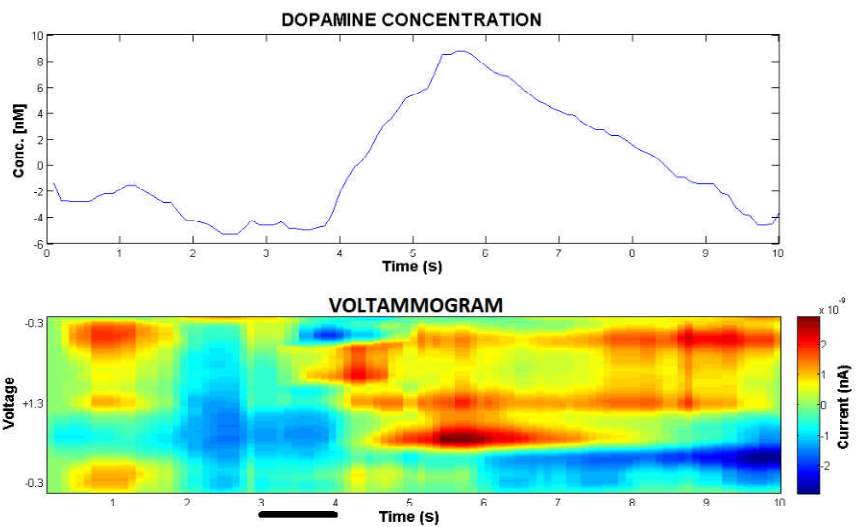


Figure 3.6: Voltammogram and dopamine concentration (day3). Stimulation at 3rd second. The timing of the stimulation is shown by a horizontal black line just below the voltammogram.

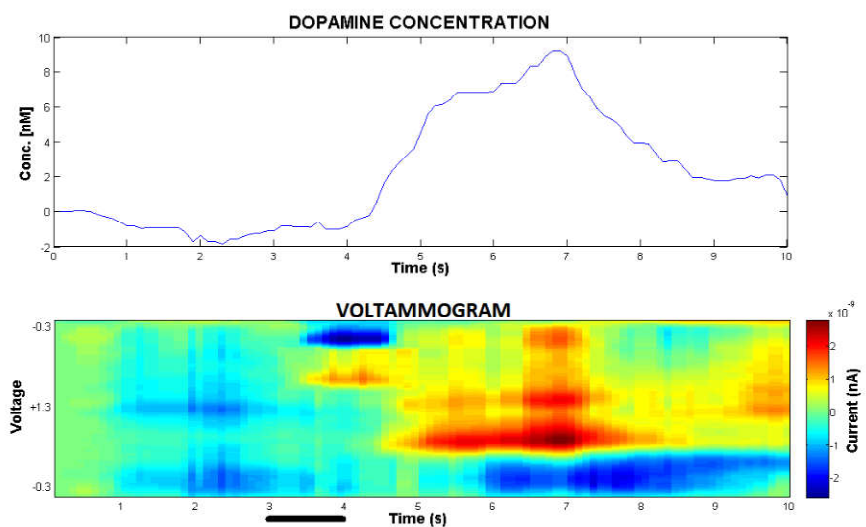


Figure 3.7: Voltammogram and dopamine concentration (day4). Stimulation at 3rd second. The timing of the stimulation is shown by a horizontal black line just below the voltammogram.

The figures shown above displays the stimulation results from the animal (Rat-2), recovered from the surgery. The concentration graphs shows the peak concentration detected in the above results around $9.5nM$ while the reuptake time is around 3 to 3.5 seconds, the cause of which can be the glial activity that delays the reuptake in the of the neurotransmitter in the parent axon terminals. Since these experiments are performed in fully awake animals, the results are noisy, which is as a result of motion artifacts, some chemical changes in the brain medium and change in pH, but still the release of dopamine is clearly visible on the respective oxidizing voltage level (0.6 Volts).

3.3 Recording During Behavioral Experiments (Pavlovian Conditioning)

In this section, the results obtained during the recordings during behavioral experiments on Rat-1. These experiments include the presentation of unexpected primary rewards (unconditioned stimuli) and reward predictive stimuli (cue light). The tasks for reward predictive stimuli is a Pavlovian conditioned approach task. The reward here is 13% Sucrose solution, $200\ \mu\text{L}$ in each delivery. For this purpose animal was kept thirsty and then training is performed followed by experimental recordings.

- **Task # 1** In this task the reward delivery is controlled by a solenoid valve. Reward is always released with a click sound produced by the solenoid. The animal is trained to response at the click sound as the reward predictor. After training, experimental recordings are performed with the release of reward at unexpected times, creating a click sound. The results with 1 trial and the average of five trials are given below:

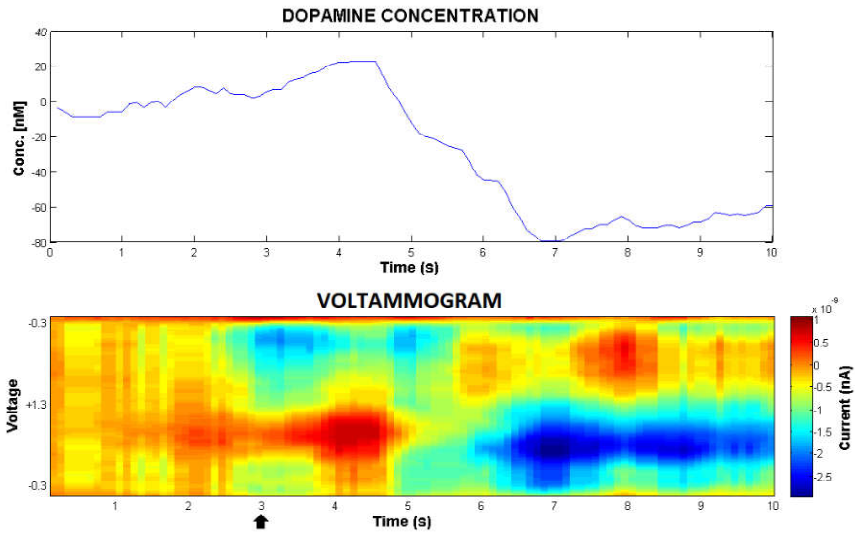


Figure 3.8: The voltammogram and dopamine concentration recorded during presentation of unexpected primary reward (i.e. sucrose solution). Reward is presented at 3rd second. Black arrow below the voltammogram shows the timing of the reward presentation.

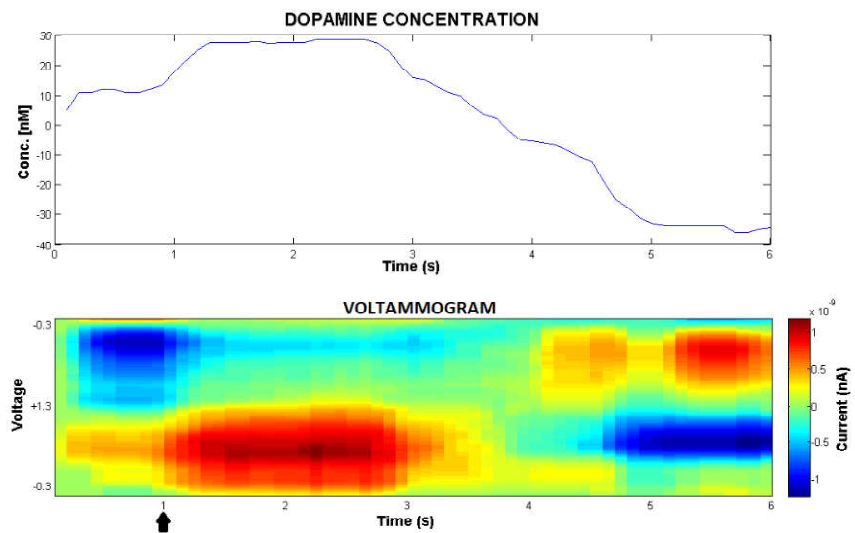


Figure 3.9: The average voltammogram and dopamine concentration based on five trials with presentation of unexpected primary rewards (i.e. sucrose solution). Rewards are presented at 1st second in all trials. Black arrow below voltammogram shows the timing of the reward presentation.

- **Task # 2** In this task, a light cue presented for 3 seconds and immediately followed by delivery of 0.2 ml of 13% sucrose solution. LED cue was the predictor of rewards. After the training for Pavlovian conditioned approach task, voltammetric signals in response to reward predictive stimuli (cue light) were recorded using the proposed system. The results with 1 trial and the average of five trials are given below:

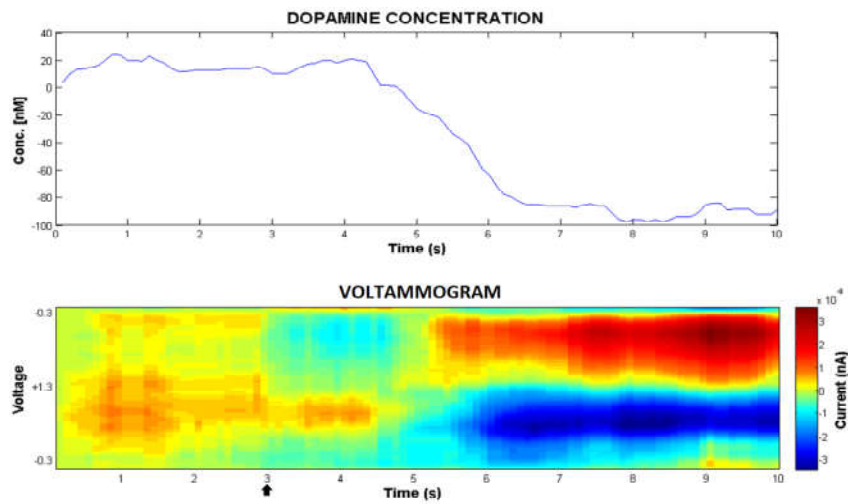


Figure 3.10: The voltammogram and dopamine concentration during presentation of a reward predictive stimulus (i.e. cue LED). The reward predictive stimulus was presented at 3rd second of the recording. Black arrow below voltammogram shows the timing of the reward predictive stimulus.

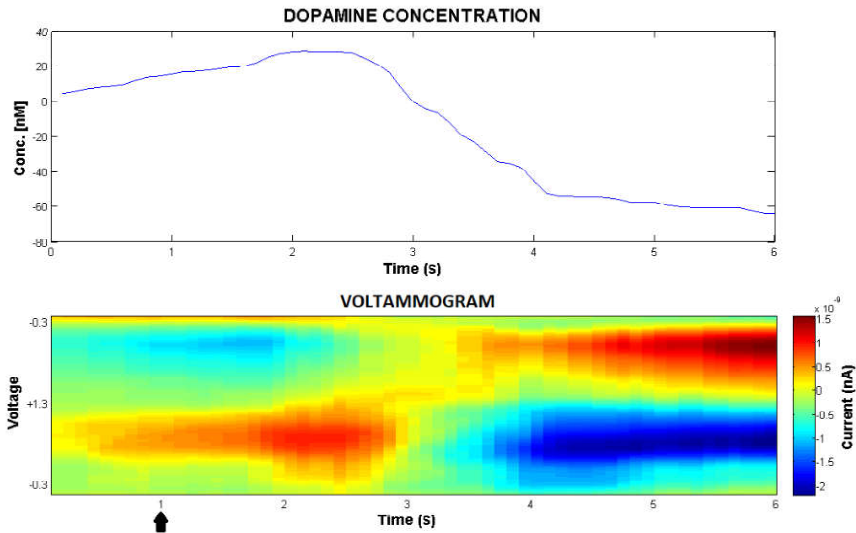


Figure 3.11: The average voltammogram and dopamine concentration based on five trials with presentation reward predictive stimuli (i.e. cue LED). The reward predictive stimuli were presented at 1st second in all trials. Black arrow below voltammogram shows the timing of the reward predictive stimuli in the trials.

In all the behavioral activities described above, the traces of dopamine have been found. The reward cue or delivery time and dates are changed to validate the reproducibility of the results. The noise was also present besides the signal but that is expected due to movement artifacts and pH change in the awake animal. Based on average of 5 recording sessions in which unexpected rewards were presented and average of 5 recording sessions in which predictive stimuli were presented (results shown above), the phasic increase in the dopamine concentration was measured as 50.5 ± 13.1 nM and 40.2 ± 13.9 nM, respectively. It is observed that the results are reproducible and are in alignment with the timings of reward cue or reward delivery. The release of dopamine in natural conditions is less than the stimulated conditions, which are visible in the results. But still the change in dopamine concentration is detectable by the system, that indicates the efficient working of the proposed system.

Chapter 4

Discussion

This thesis proposes and implements a lab built voltammetric system that is used to acquire chronic dopamine recordings from the ventromedial striatum of the rat brain. This system, comprising hardware and software components, is capable of detecting dopamine release with high temporal resolution (10 Hz). The hardware is divided into voltammetric signal generator, current to voltage converter and DAQ system. Voltammetric signal generated here is actually a triangular waveform having voltage range from -0.4 to +1.3 V (having the rising and falling slopes of 400 V/s) appearing after every 100 *ms*. For the wave generation, pulse of 8.7*ms* is generated by PIC micro controller unit (MCU) and is fed into the integrator followed by summing amplifier, the integrator integrates the pulse and produces triangular wave, resistors and capacitors are used to adjust the ramp of the triangle. The main purpose of summing amplifier is to adjust the offset and gain of the output waveform. The use of voltage follower is made to support the signal strength. Optocoupler is used to isolate the MCU from the integrator circuit to avoid the noise due to clock frequency of the MCU. Phase locking feature is used to generate the voltammetric wave which eradicates the effect of the mains line noise in the subtracted signal.

The waveform generated is input to the current to voltage converter that detects the current change on the electrode surface and converts it into voltage. Whenever there is dopamine release near the electrode, it is oxidized and the current generated by it is converted into voltage by current to voltage converter. Finally DAQ system, consisting of DAQ card (from National Instruments), receives the signal from current to voltage converter and feeds it to the computer.

The software part consists of a program created on Lab-view environment. The data is acquired at 200 kHz frequency with 3000 samples in each cycle. The acquisition is triggered by the pulse appearing after every 100 ms. The acquired data consists of both baseline and dopamine signal cycles. The data is accumulated in an array and filter is applied. After filtering the data, baseline signal is subtracted from dopamine signal getting the concentration of dopamine released. The proposed program is capable of displaying the results (concentration) in the form of graph and voltammogram, and is also able to store it for later use.

To validate the system, chronic implantations are made in ventro medial striatum (VMS) particularly to the NAc. For this purpose carbon fiber microsensors (carbon fiber in fused silica capillary covered by polyimide) along with stimulation electrodes (tungsten coated with polyimide) and reference electrodes (Ag/AgCl) are implanted on Sprague Dawley male rats (weight = 300-400 g; age = 3-6 months). After the recovery period (1 month), rats are trained for reward predictive stimuli (LED cue). Experiments are performed, both with stimulations and behavioral tasks (unexpected rewards and reward predictive stimuli) resulting in the observation of phasic increase in dopamine.

The results shown in Figure 3.2 and Figure 3.3 are of electrical stimulation experiments recorded during the surgery of Rat-1. The peak concentration measured during these recordings was 132.8 *nM* and the reuptake time is observed to be around 1.25 *seconds*. The stimulation experiments performed on Rat-2 after it's recovery from the surgery are shown in Figure 3.4 to Figure 3.7. The

change in dynamics of the system can be observed, the decrease in the slope of dopamine release as compared to that of the recordings during the surgery is indicating the effect of glial activity around the electrode that may be inhibiting or slowing down the dopamine molecules to reach at the electrode surface. This detected change is establishing the fact that the proposed system is robust enough to even detect such changes. The peak concentration value detected during the electrical stimulation after the surgery is found to be $9.5nM$. Since the animal used here is different (i.e. Rat-2) and due to different surface condition of the carbon fiber, the reuptake time is different as compared to that of Rat-1 which in this case is around 3 *seconds*. Figure ?? to Figure 3.11 represents the results of the recordings during behavioral experiments, these experiments include the unexpected release of primary reward and reward predictive stimuli. For these tasks, the animal (Rat-1) is kept thirsty for 24 hours and then the experiments are performed. The increase in dopamine concentration is observed just after the delivery of unexpected reward as shown in Figure ?? to Figure 3.9. The concentration measured on the basis of 5 trials is about $50.5 \pm 13.1 nM$. Further, the same animal (Rat-1) is trained to respond on Pavlovian task, in this task cue LED turns On as a predictor of reward and the reward is delivered 3 seconds after the cue appears. Recordings are performed after training the animal. The results shown in Figure 3.10 to Figure 3.11 are recorded when the rat was performing the above described task. The increase in dopamine concentration can be seen on the delivery of the cue rather than the delivery of reward, which is supporting previous researches. One more thing which can be observed in the behavioral experiments is the artifact due to pH change that appears after the release of dopamine. This pH noise is able to bury some small dopamine signal and needs to be removed, this matter is discussed later in the future work. The dopamine concentration in reward predictive stimuli experiments based on 5 trials is $40.2 \pm 13.9 nM$.

Some other experiments are performed in which the animal is trained to press the lever when the cue LED turns ON in order to get the reward, in those experiments, the dopamine release is realized at the availability of the cue, and there

was no such change notice during the lever pressing. This paradigm needs to be validated with more trials in the future.

Our results based on the recordings from rat brain indicate that phasic increases in dopamine concentration in the VMS in response to electrical stimulation, delivery of unexpected rewards and reward predictive stimuli can be detected using chronically implanted carbon fiber microsensors and therefore validating the robustness of the proposed voltammetric system we developed.

4.1 Advantages of the System

The proposed system is a cost effective solution (cost around \$ 1200) as compared to the expensive systems commercially available in the market. The maintenance of the system is easy and affordable, and a person with some knowledge of electrical circuits and Lab-view will be able to manage it. Besides the above basic advantages, filters and opto-couplers are used in this system to exterminate any high frequency noise either from mains line or clock frequency noise. Since this system (hardware and software) is developed in lab, it has an option of being modified anytime depending upon the requirements of the user and experiments that are to be performed. These modifications may include change in characteristics of the wave, change in GUI, external triggering of different paradigms and different storage options.

4.2 Limitations of the System and Future Improvements

In addition to the advantages, there are some limitations in this system. One of them is that the system has a wired setup that restricts the movement of animal. The wires connected to the headstage may affect the experiments in awake animals. This issue can be addressed by converting the system into a wireless system that will allow some degree of freedom to the subject and can decrease the noise due to wire stretching or twisting. One more limitation of the system is its inability to remove the movement artifacts and pH changes that appear in awake animals. These artifacts can be seen in Figure 3.4 to Figure 3.11. Sometimes the pH change can be large and can coincide with the dopamine resulting in loss of little changes in dopamine concentration. Some machine learning algorithms like PCA (Principle Component Analysis) and PLSR (Partial Least Square Regression) can be used to separate the dopamine signal from the artifacts caused by the pH change. The other future improvement can be to make it an online recording and display system that can show the subtracted signal in real time rather than storing the data and then processing it offline.

Bibliography

- [1] R. Karaman, “Prodrugs design based on inter- and intramolecular processes,” pp. 1–76, 07 2014.
- [2] K. M. Money and G. D. Stanwood, “Developmental origins of brain disorders: roles for dopamine,” *Frontiers in cellular neuroscience*, vol. 7, p. 260, 2013.
- [3] L. W. Hung, S. Neuner, J. S. Polepalli, K. T. Beier, M. Wright, J. J. Walsh, E. M. Lewis, L. Luo, K. Deisseroth, G. Dölen, *et al.*, “Gating of social reward by oxytocin in the ventral tegmental area,” *Science*, vol. 357, no. 6358, pp. 1406–1411, 2017.
- [4] R. A. Depue, M. Luciana, P. Arbisi, P. Collins, and A. Leon, “Dopamine and the structure of personality: Relation of agonist-induced dopamine activity to positive emotionality,” *Journal of Personality and Social Psychology*, vol. 67, no. 3, p. 485, 1994.
- [5] J. Wacker, M.-L. Chavanon, and G. Stemmler, “Investigating the dopaminergic basis of extraversion in humans: A multilevel approach,” *Journal of Personality and Social Psychology*, vol. 91, no. 1, p. 171, 2006.
- [6] A. B. Barron, E. Søvik, and J. L. Cornish, “The roles of dopamine and related compounds in reward-seeking behavior across animal phyla,” *Frontiers in behavioral neuroscience*, vol. 4, p. 163, 2010.
- [7] C. A. Owesson-White, J. F. Cheer, M. Beyene, R. M. Carelli, and R. M. Wightman, “Dynamic changes in accumbens dopamine correlate with learning during intracranial self-stimulation,” *Proceedings of the National Academy of Sciences*, vol. 105, no. 33, pp. 11957–11962, 2008.

- [8] J. J. Day, M. F. Roitman, R. M. Wightman, and R. M. Carelli, “Associative learning mediates dynamic shifts in dopamine signaling in the nucleus accumbens,” *Nature neuroscience*, vol. 10, no. 8, p. 1020, 2007.
- [9] J. Mirenowicz and W. Schultz, “Importance of unpredictability for reward responses in primate dopamine neurons,” *Journal of neurophysiology*, vol. 72, no. 2, pp. 1024–1027, 1994.
- [10] G. Planz, G. Wiethold, E. Appel, D. Böhmer, D. Palm, and H. Grobecker, “Correlation between increased dopamine- β -hydroxylase activity and catecholamine concentration in plasma: Determination of acute changes in sympathetic activity in man,” *European journal of clinical pharmacology*, vol. 8, no. 3-4, pp. 181–188, 1975.
- [11] N. Weiner, “Tyrosine-3-monooxygenase (tyrosine hydroxylase),” *Aromatic amino acid hydroxylases and mental disease*, pp. 141–190, 1979.
- [12] M. Jaber, S. W. Robinson, C. Missale, and M. G. Caron, “Dopamine receptors and brain function,” *Neuropharmacology*, vol. 35, no. 11, pp. 1503–1519, 1996.
- [13] C. De Mei, M. Ramos, C. Iitaka, and E. Borrelli, “Getting specialized: presynaptic and postsynaptic dopamine d2 receptors,” *Current opinion in pharmacology*, vol. 9, no. 1, pp. 53–58, 2009.
- [14] A. Barbeau, “The pathogenesis of parkinson’s disease: a new hypothesis,” *Canadian Medical Association Journal*, vol. 87, no. 15, p. 802, 1962.
- [15] N. D. Volkow, G.-J. Wang, J. S. Fowler, J. Logan, M. Jayne, D. Franceschi, C. Wong, S. J. Gatley, A. N. Gifford, Y.-S. Ding, *et al.*, “nonhedonic food motivation in humans involves dopamine in the dorsal striatum and methylphenidate amplifies this effect,” *Synapse*, vol. 44, no. 3, pp. 175–180, 2002.
- [16] S. Robinson, A. J. Rainwater, T. S. Hnasko, and R. D. Palmiter, “Viral restoration of dopamine signaling to the dorsal striatum restores instrumental conditioning to dopamine-deficient mice,” *Psychopharmacology*, vol. 191, no. 3, pp. 567–578, 2007.

- [17] R. I. Weiner and W. F. Ganong, “Role of brain monoamines and histamine in regulation of anterior pituitary secretion.,” *Physiological Reviews*, vol. 58, no. 4, pp. 905–976, 1978.
- [18] M. Puig, J. Rose, R. Schmidt, and N. Freund, “Dopamine modulation of learning and memory in the prefrontal cortex: insights from studies in primates, rodents, and birds,” *Frontiers in neural circuits*, vol. 8, p. 93, 2014.
- [19] L. Harsing Jr, “Dopamine and the dopaminergic systems of the brain,” in *Handbook of Neurochemistry and Molecular Neurobiology*, pp. 149–170, Springer, 2008.
- [20] M. F. Roitman, G. D. Stuber, P. E. Phillips, R. M. Wightman, and R. M. Carelli, “Dopamine operates as a subsecond modulator of food seeking,” *Journal of Neuroscience*, vol. 24, no. 6, pp. 1265–1271, 2004.
- [21] W. Schultz, P. Dayan, and P. R. Montague, “A neural substrate of prediction and reward,” *Science*, vol. 275, no. 5306, pp. 1593–1599, 1997.
- [22] R. A. Wise, “Brain reward circuitry: insights from unsensed incentives,” *Neuron*, vol. 36, no. 2, pp. 229–240, 2002.
- [23] A. M. Graybiel, T. Aosaki, A. W. Flaherty, and M. Kimura, “The basal ganglia and adaptive motor control,” *Science*, vol. 265, no. 5180, pp. 1826–1831, 1994.
- [24] A. Tsui and O. Isacson, “Functions of the nigrostriatal dopaminergic synapse and the use of neurotransplantation in parkinsons disease,” *Journal of neurology*, vol. 258, no. 8, p. 1393, 2011.
- [25] H. Bernheimer, W. Birkmayer, O. Hornykiewicz, K. Jellinger, and F. . Seitelberger, “Brain dopamine and the syndromes of parkinson and huntington clinical, morphological and neurochemical correlations,” *Journal of the neurological sciences*, vol. 20, no. 4, pp. 415–455, 1973.
- [26] M. Goldstein, A. Battista, T. Ohmoto, B. Anagnoste, and K. Fuxe, “Tremor and involuntary movements in monkeys: effect of l-dopa and of a dopamine receptor stimulating agent,” *Science*, vol. 179, no. 4075, pp. 816–817, 1973.

- [27] C. Gross, “Neuronal activity of area 4 and movement parameters recorded in trained monkeys after unilateral lesion of the substantia nigra,” *Experimental Brain Research*, vol. 7, pp. 181–193, 1983.
- [28] A. Carlsson, B. Falck, and N.-Å. Hillarp, “Cellular localization of brain monoamines,” *Acta physiologica Scandinavica. Supplementum*, vol. 56, no. 196, p. 1, 1962.
- [29] P. Keller and W. Lichtensteiger, “Stimulation of tubero-infundibular dopamine neurones and gonadotrophin secretion,” *The Journal of physiology*, vol. 219, no. 2, pp. 385–401, 1971.
- [30] H. Schneider and S. McCann, “Possible role of dopamine as transmitter to promote discharge of lh-releasing factor,” *Endocrinology*, vol. 85, no. 1, pp. 121–132, 1969.
- [31] P.-P. Rompré and R. A. Wise, “Behavioral evidence for midbrain dopamine depolarization inactivation,” *Brain research*, vol. 477, no. 1-2, pp. 152–156, 1989.
- [32] N. D. Volkow, G.-J. Wang, J. S. Fowler, and Y.-S. Ding, “Imaging the effects of methylphenidate on brain dopamine: new model on its therapeutic actions for attention-deficit/hyperactivity disorder,” *Biological psychiatry*, vol. 57, no. 11, pp. 1410–1415, 2005.
- [33] G. Winterer and D. R. Weinberger, “Genes, dopamine and cortical signal-to-noise ratio in schizophrenia,” *Trends in neurosciences*, vol. 27, no. 11, pp. 683–690, 2004.
- [34] L. A. Sombers, M. Beyene, R. M. Carelli, and R. M. Wightman, “Synaptic overflow of dopamine in the nucleus accumbens arises from neuronal activity in the ventral tegmental area,” *Journal of Neuroscience*, vol. 29, no. 6, pp. 1735–1742, 2009.
- [35] F. Cacciapaglia, R. M. Wightman, and R. M. Carelli, “Rapid dopamine signaling differentially modulates distinct microcircuits within the nucleus accumbens during sucrose-directed behavior,” *Journal of Neuroscience*, vol. 31, no. 39, pp. 13860–13869, 2011.

- [36] B. T. Chen, F. W. Hopf, and A. Bonci, “Synaptic plasticity in the mesolimbic system,” *Annals of the New York Academy of Sciences*, vol. 1187, no. 1, pp. 129–139, 2010.
- [37] W. Schultz, “Predictive reward signal of dopamine neurons,” *Journal of neurophysiology*, vol. 80, no. 1, pp. 1–27, 1998.
- [38] J. Mirenowicz and W. Schultz, “Preferential activation of midbrain dopamine neurons by appetitive rather than aversive stimuli,” *Nature*, vol. 379, no. 6564, p. 449, 1996.
- [39] H. O. Pettit and J. B. Justice Jr, “Effect of dose on cocaine self-administration behavior and dopamine levels in the nucleus accumbens,” *Brain research*, vol. 539, no. 1, pp. 94–102, 1991.
- [40] M. C. Ritz, R. Lamb, M. Kuhar, *et al.*, “Cocaine receptors on dopamine transporters are related to self-administration of cocaine,” *Science*, vol. 237, no. 4819, pp. 1219–1223, 1987.
- [41] J. Millar and T. Barnett, “Basic instrumentation for fast cyclic voltammetry,” *Journal of neuroscience methods*, vol. 25, no. 2, pp. 91–95, 1988.
- [42] J. A. Stamford, P. Palij, C. Davidson, C. M. Jorm, and J. Millar, “Simultaneous real-time electrochemical and electrophysiological recording in brain slices with a single carbon-fibre microelectrode,” *Journal of neuroscience methods*, vol. 50, no. 3, pp. 279–290, 1993.
- [43] P. Takmakov, M. K. Zachek, R. B. Keithley, E. S. Bucher, G. S. McCarty, and R. M. Wightman, “Characterization of local pH changes in brain using fast-scan cyclic voltammetry with carbon microelectrodes,” *Analytical chemistry*, vol. 82, no. 23, pp. 9892–9900, 2010.
- [44] P. Hashemi, E. C. Dankoski, J. Petrovic, R. B. Keithley, and R. Wightman, “Voltammetric detection of 5-hydroxytryptamine release in the rat brain,” *Analytical chemistry*, vol. 81, no. 22, pp. 9462–9471, 2009.
- [45] J. Park, B. M. Kile, and R. Mark Wightman, “In vivo voltammetric monitoring of norepinephrine release in the rat ventral bed nucleus of the stria

- terminalis and anteroventral thalamic nucleus,” *European Journal of Neuroscience*, vol. 30, no. 11, pp. 2121–2133, 2009.
- [46] D. R. Humphrey and E. M. Schmidt, “Extracellular single-unit recording methods,” in *Neurophysiological techniques*, pp. 1–64, Springer, 1990.
- [47] D. L. Robinson, B. J. Venton, M. L. Heien, and R. M. Wightman, “Detecting subsecond dopamine release with fast-scan cyclic voltammetry in vivo,” *Clinical chemistry*, vol. 49, no. 10, pp. 1763–1773, 2003.
- [48] D. Michael, E. R. Travis, and R. M. Wightman, “Peer reviewed: color images for fast-scan cv measurements in biological systems,” *Analytical chemistry*, vol. 70, no. 17, pp. 586A–592A, 1998.
- [49] J. O. Howell and R. M. Wightman, “Ultrafast voltammetry and voltammetry in highly resistive solutions with microvoltammetric electrodes,” *Analytical Chemistry*, vol. 56, no. 3, pp. 524–529, 1984.
- [50] M. V. Mirkin, L. O. Bulhoes, and A. J. Bard, “Determination of the kinetic parameters for the electroreduction of fullerene c60 by scanning electrochemical microscopy and fast scan cyclic voltammetry,” *Journal of the American Chemical Society*, vol. 115, no. 1, pp. 201–204, 1993.
- [51] R. M. Wightman and D. O. Wipf, “High-speed cyclic voltammetry,” *Accounts of Chemical Research*, vol. 23, no. 3, pp. 64–70, 1990.
- [52] A. S. Khan and A. C. Michael, “Invasive consequences of using microelectrodes and microdialysis probes in the brain,” *TrAC Trends in Analytical Chemistry*, vol. 22, no. 8, pp. 503–508, 2003.
- [53] K. Pihel, Q. D. Walker, and R. M. Wightman, “Overoxidized polypyrrole-coated carbon fiber microelectrodes for dopamine measurements with fast-scan cyclic voltammetry,” *Analytical chemistry*, vol. 68, no. 13, pp. 2084–2089, 1996.

- [54] J. X. Feng, M. Brazell, K. Renner, R. Kasser, and R. N. Adams, "Electrochemical pretreatment of carbon fibers for in vivo electrochemistry: effects on sensitivity and response time," *Analytical chemistry*, vol. 59, no. 14, pp. 1863–1867, 1987.
- [55] S. Hafizi, Z. L. Kruk, and J. A. Stamford, "Fast cyclic voltammetry: improved sensitivity to dopamine with extended oxidation scan limits," *Journal of neuroscience methods*, vol. 33, no. 1, pp. 41–49, 1990.
- [56] R. D. O'Neill and J. P. Lowry, "On the significance of brain extracellular uric acid detected with in-vivo monitoring techniques: a review," *Behavioural brain research*, vol. 71, no. 1-2, pp. 33–49, 1995.
- [57] M. M. Iravani, J. Millar, and Z. L. Kruk, "Differential release of dopamine by nitric oxide in subregions of rat caudate putamen slices," *Journal of neurochemistry*, vol. 71, no. 5, pp. 1969–1977, 1998.
- [58] P. L. Runnels, J. D. Joseph, M. J. Logman, and R. M. Wightman, "Effect of pH and surface functionalities on the cyclic voltammetric responses of carbon-fiber microelectrodes," *Analytical chemistry*, vol. 71, no. 14, pp. 2782–2789, 1999.
- [59] G. A. Gerhardt and A. F. Hoffman, "Effects of recording media composition on the responses of nafion-coated carbon fiber microelectrodes measured using high-speed chronoamperometry," *Journal of neuroscience methods*, vol. 109, no. 1, pp. 13–21, 2001.
- [60] M. F. Roitman, R. A. Wheeler, R. M. Wightman, and R. M. Carelli, "Real-time chemical responses in the nucleus accumbens differentiate rewarding and aversive stimuli," *Nature neuroscience*, vol. 11, no. 12, p. 1376, 2008.
- [61] J. O. Gan, M. E. Walton, and P. E. Phillips, "Dissociable cost and benefit encoding of future rewards by mesolimbic dopamine," *Nature neuroscience*, vol. 13, no. 1, p. 25, 2010.
- [62] G. A. Gerhardt, C. Ksir, C. Pivik, S. D. Dickinson, J. Sabeti, and N. R. Zahner, "Methodology for coupling local application of dopamine and other

chemicals with rapid in vivo electrochemical recordings in freely-moving rats,” *Journal of neuroscience methods*, vol. 87, no. 1, pp. 67–76, 1999.

[63] A. H. Swiergiel, V. S. Palamarchouk, and A. J. Dunn, “A new design of carbon fiber microelectrode for in vivo voltammetry using fused silica,” *Journal of neuroscience methods*, vol. 73, no. 1, pp. 29–33, 1997.

[64] J. J. Clark, S. G. Sandberg, M. J. Wanat, J. O. Gan, E. A. Horne, A. S. Hart, C. A. Akers, J. G. Parker, I. Willuhn, V. Martinez, *et al.*, “Chronic microsensors for longitudinal, subsecond dopamine detection in behaving animals,” *Nature methods*, vol. 7, no. 2, p. 126, 2010.

Appendix A

Appendix

A.1 Amplifier Schematic

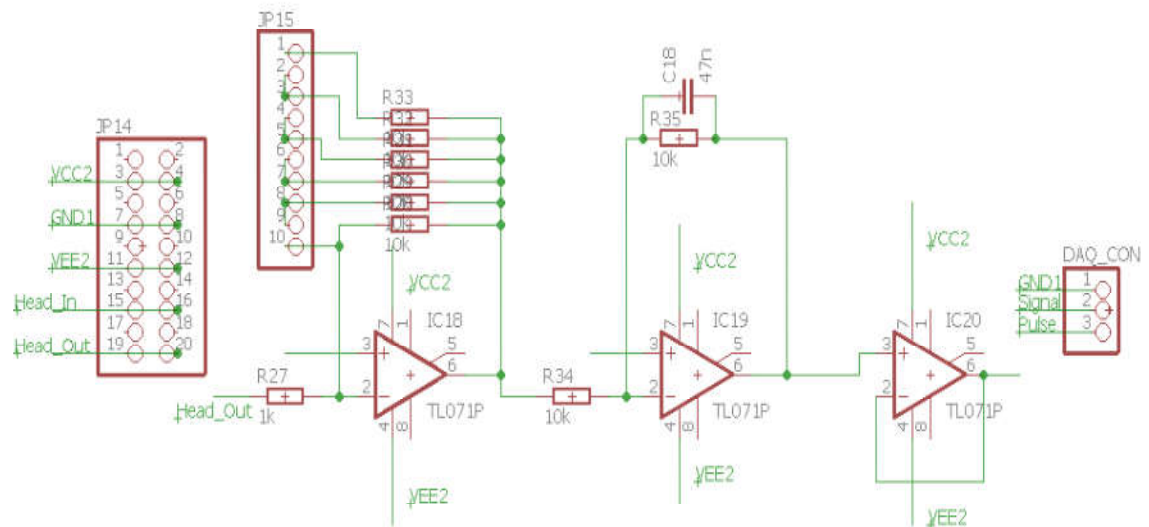


Figure A.1: Schematic of the amplifier circuit connected after headstage

A.2 Pulse Generator Schematic

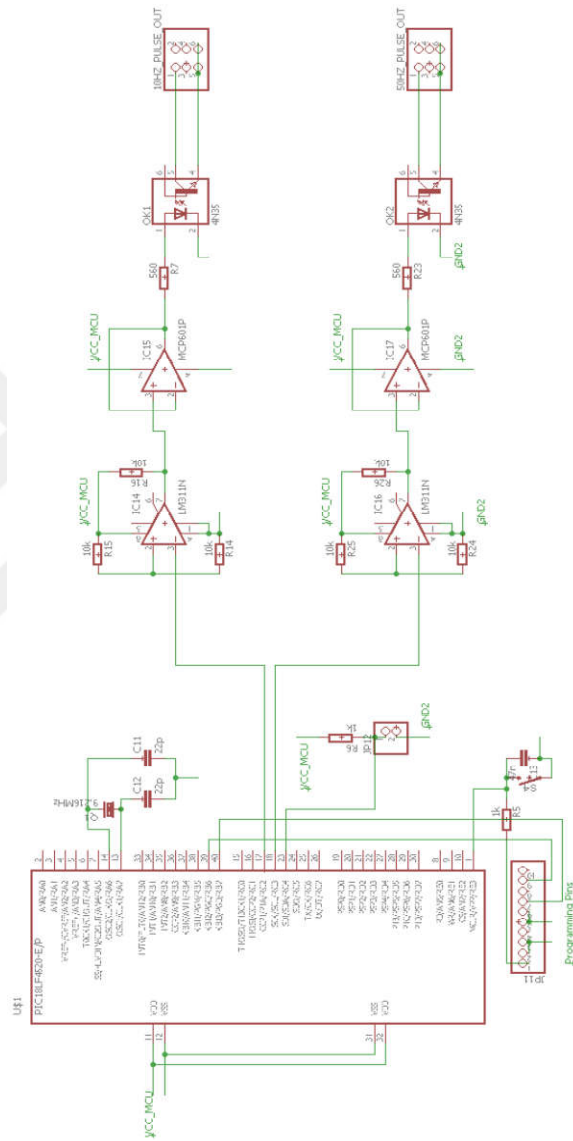


Figure A.2: Schematic of the pulse generator circuit

A.3 Integrator Schematic

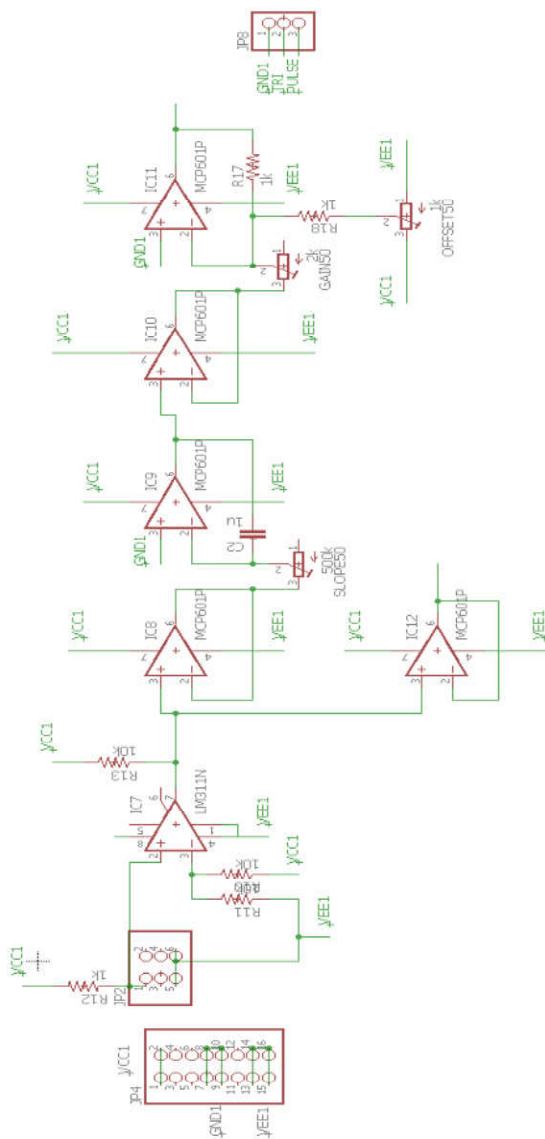


Figure A.3: Schematic of the integrator circuit

DESIGN OF A VOLTAMMETRY SYSTEM FOR IN VIVO MEASUREMENTS OF DOPAMINE CONCENTRATION

ORIGINALITY REPORT

6%

SIMILARITY INDEX

4%

INTERNET SOURCES

3%

PUBLICATIONS

2%

STUDENT PAPERS

PRIMARY SOURCES

- 1** Submitted to Nashville State Community College
Student Paper 1%
- 2** changingminds.org
Internet Source <1%
- 3** Submitted to Bilkent University
Student Paper <1%
- 4** www.dsv.kth.se
Internet Source <1%
- 5** etd.lib.metu.edu.tr
Internet Source <1%
- 6** Elizabeth S. Bucher, Kenneth Brooks, Matthew D. Verber, Richard B. Keithley et al. "Flexible Software Platform for Fast-Scan Cyclic Voltammetry Data Acquisition and Analysis", *Analytical Chemistry*, 2013
Publication <1%
- 7** James A. Dickson. "Tris (2,2'-